

## LA-UR-21-26806

Approved for public release; distribution is unlimited.

Title: Assessment of double shell ablator asymmetry sources and shape control

Author(s): Sacks, Ryan Foster  
Loomis, Eric Nicholas  
Keiter, Paul Arthur  
Robey, Harry F. III

Intended for: Report

Issued: 2021-07-15

---

**Disclaimer:**

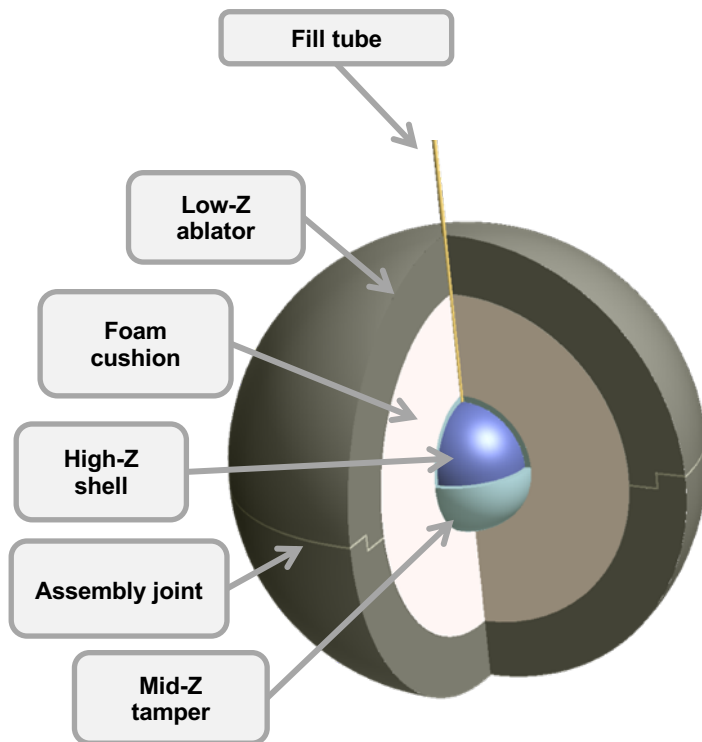
Los Alamos National Laboratory, an affirmative action/equal opportunity employer, is operated by Triad National Security, LLC for the National Nuclear Security Administration of U.S. Department of Energy under contract 89233218CNA000001. By approving this article, the publisher recognizes that the U.S. Government retains nonexclusive, royalty-free license to publish or reproduce the published form of this contribution, or to allow others to do so, for U.S. Government purposes. Los Alamos National Laboratory requests that the publisher identify this article as work performed under the auspices of the U.S. Department of Energy. Los Alamos National Laboratory strongly supports academic freedom and a researcher's right to publish; as an institution, however, the Laboratory does not endorse the viewpoint of a publication or guarantee its technical correctness.

# Assessment of double shell ablator asymmetry sources and shape control

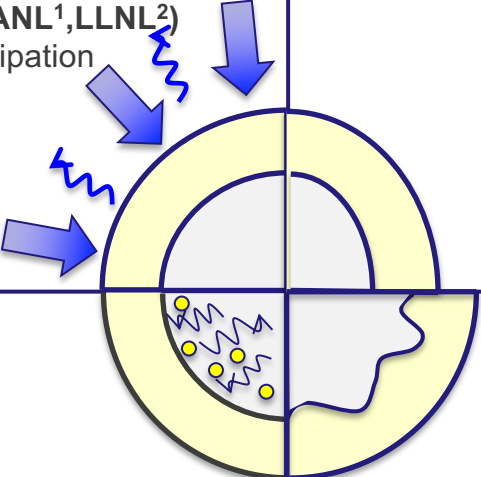
## L2 Milestone Review

Ryan Sacks, Eric Loomis, Paul Keiter,  
Harry Robey  
for LANL double shell team

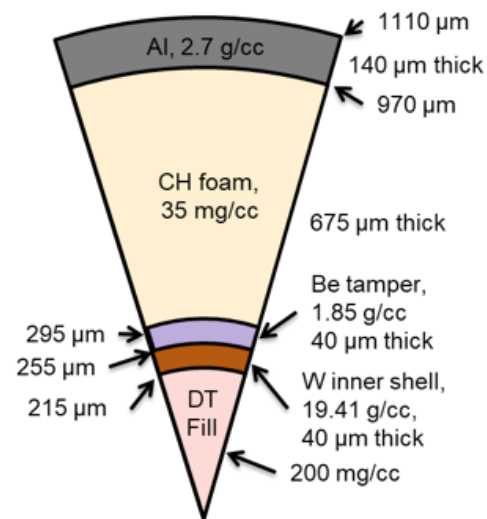
July 14, 2021



# We have a work break-down framework for addressing key gaps in multi-shell physics

Target Driver coupling	Shape Transfer
<ul style="list-style-type: none"> <li>Indirect Drive (LANL<sup>1</sup>, LLNL<sup>2</sup>)</li> <li>Foam energy dissipation</li> <li>LPI</li> </ul>	<ul style="list-style-type: none"> <li>Sources of asymmetries                             <ul style="list-style-type: none"> <li>Hohlraum/Laser drive</li> <li>Joint/shell offset</li> <li>Foam density</li> </ul> </li> </ul>
 <ul style="list-style-type: none"> <li>Diffusion of High-Z materials into gas</li> <li>High/Low Z mix</li> <li>Radiation Trapping Efficiency</li> </ul>	<ul style="list-style-type: none"> <li>Defect Hydro                             <ul style="list-style-type: none"> <li>Joint + Fill tube</li> </ul> </li> <li>Convergence effects</li> <li>Stability of inner shell</li> </ul>
Radiation Trapping/Kinetics/Burn	Inner shell stability

## LANL point design

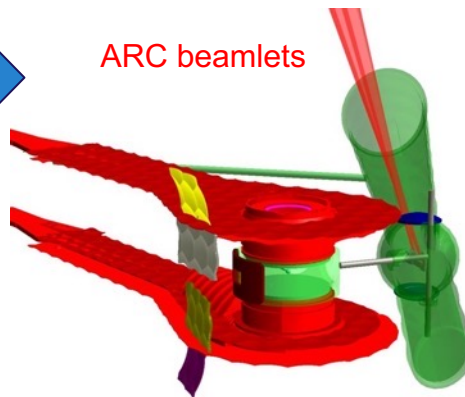
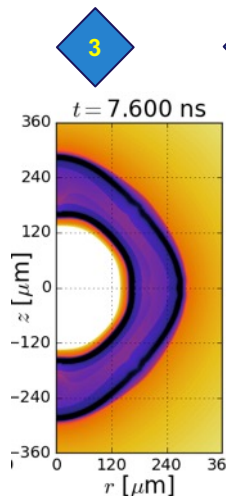
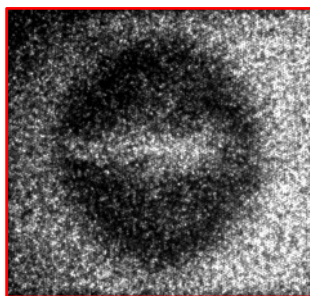


<sup>1</sup>E. Merritt et al Physics of Plasmas **26**, 052702 (2019)

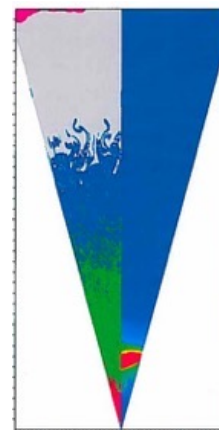
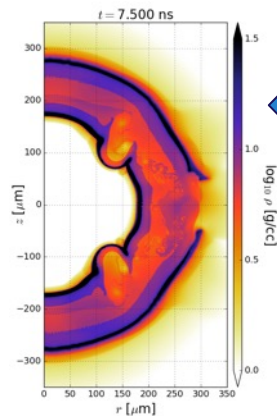
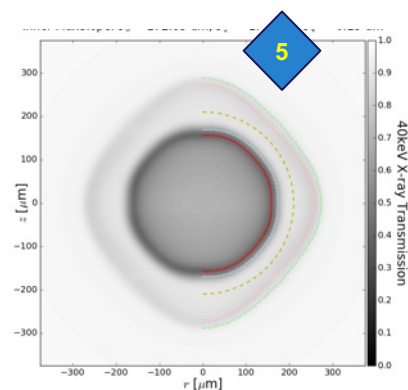
<sup>2</sup>Y. Ping et al., Nature Physics (2018)

# An L2 milestone schedule was submitted to NNSA in 2020 based on our 5-year development plan

FY21	FY22	FY23
L2 milestone schedule		



ARC beamlets



Inner shell stability

## ➤ L2 Milestones (double shell platforms and physics)

1. [Q3 FY21] outer shell symmetry control
2. [Q4 FY21] Ablator joint feature modeling validation
3. [Q1 FY22] Predicted sensitivities to low/mid-mode inner shell shape
4. [Q2 FY22] ARC high-energy radiograph demonstration of full double shell
5. [Q4 FY23] demonstration of inner shell shape transfer control
6. [Q4 FY23] evaluation of graded density pusher for mix control

# This L2 milestone definition and assessment approach

## Definition:

- **Complete assessment of outer-shell shape asymmetry, including identification of sources and quantification of control.**
- **Measurements of outer shell shape are evaluated and compared with known and suspected sources of asymmetry**
- **Panel evaluation of the completeness of the analysis and identify unconsidered sources of asymmetry**

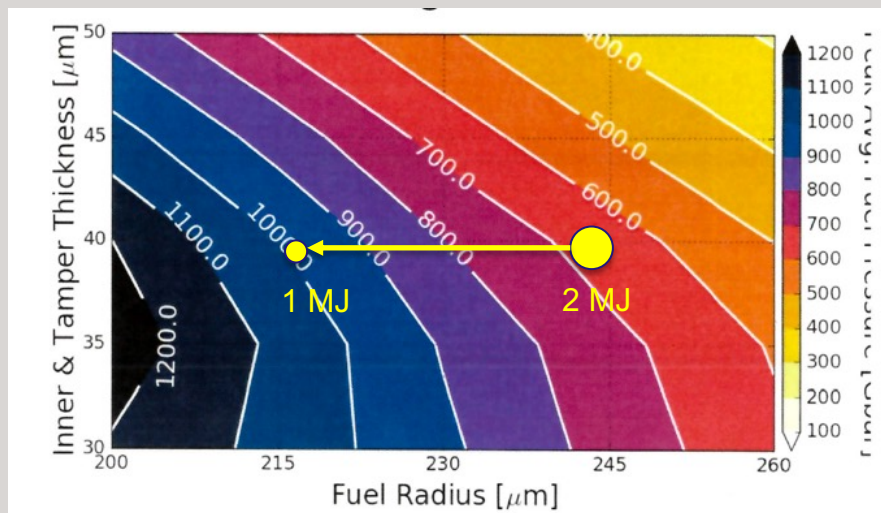
## Approach:

- **HYDRA integrated hohlraum/capsule simulation sensitivities to asymmetry sources (Loomis)**
- **Comparison of shape data to current best hohlraum model HYDRA postshots (Sacks, Keiter, Robey)**

# LANL point design double shell trades-off high 1D yield for robustness against asymmetries

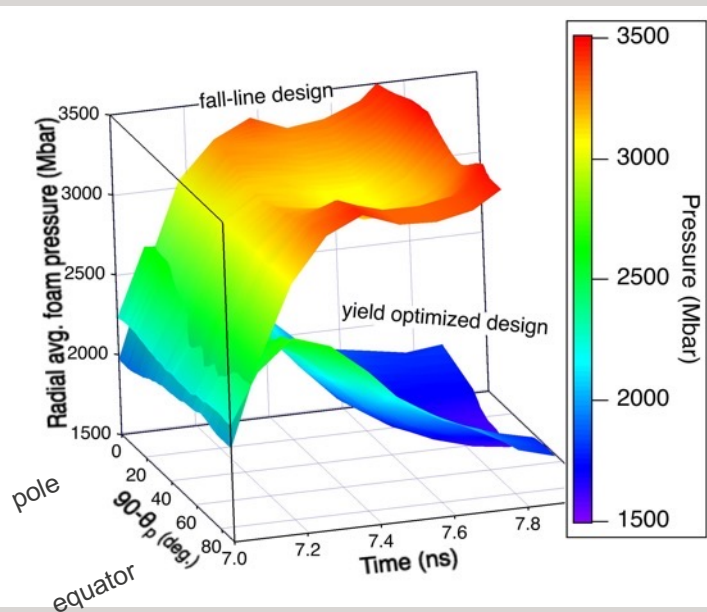
Decrease fuel volume to increase stagnation pressure and temperature

xRAGE simulations J. Sauppe



Best fall line ← Higher 1D yield

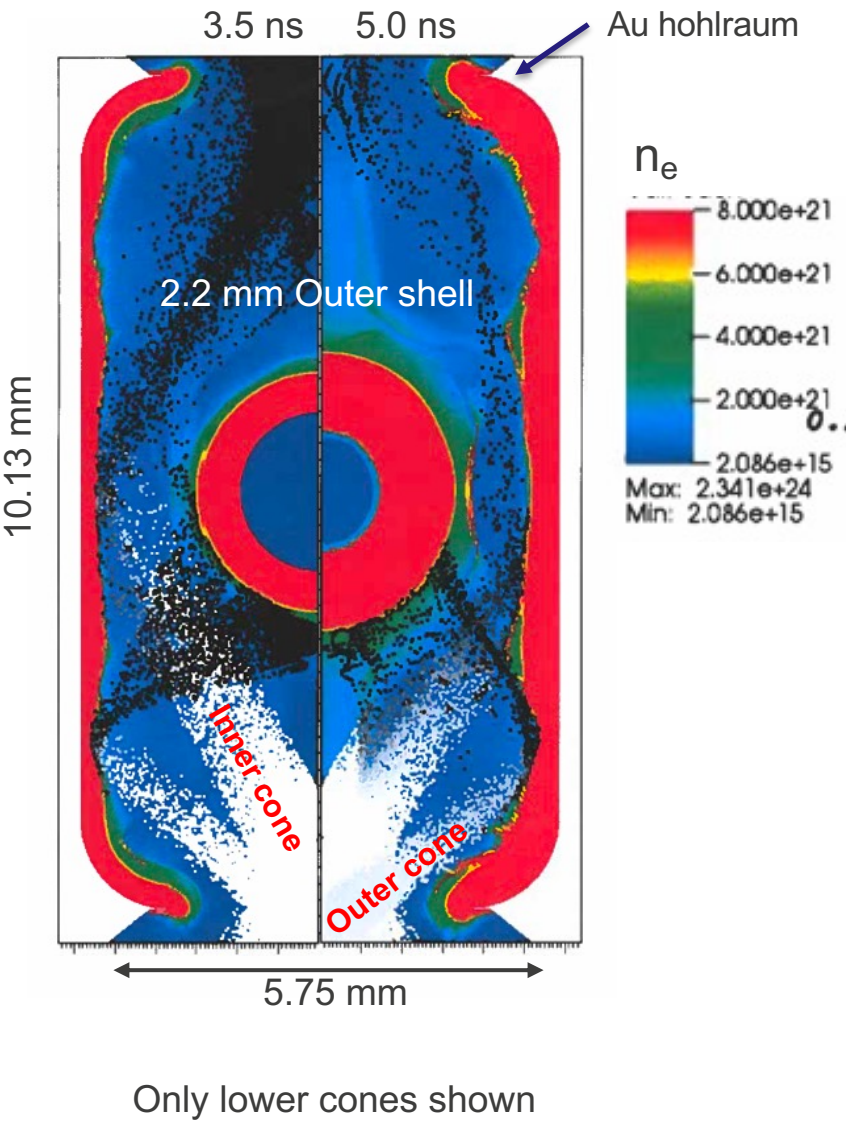
Shell collision at smaller radius increases foam pressure 'kick' to inner shell



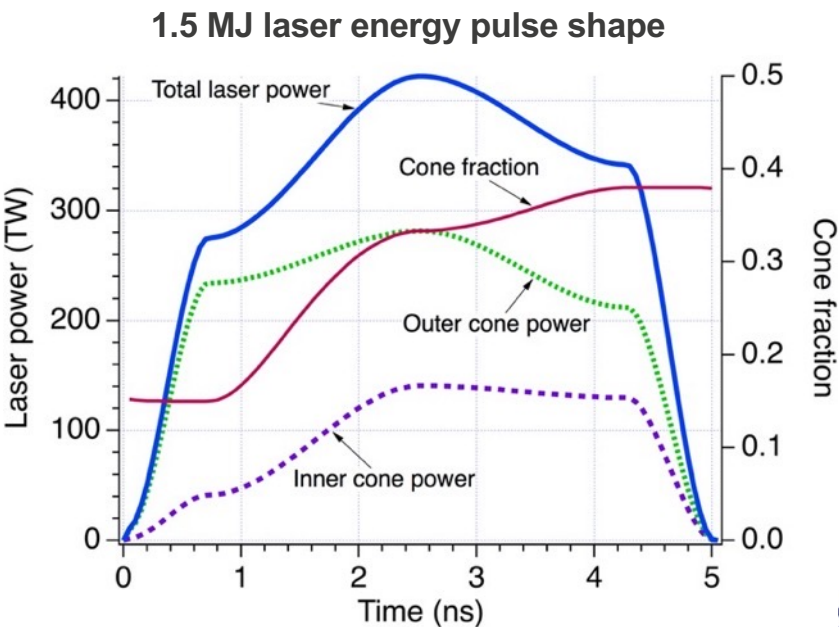
- High stagnation pressure and high, sustained collision foam pressure leads to 'upstream' burn, which reduces time for asymmetries to perturb fuel



# Hohlraum low-mode asymmetries mostly come from non-optimal laser cone pointing and laser power balance



- Hohlraum asymmetry sources
- Pulse shape (CF vs time)
  - Beam pointing
  - Hohlraum fill density
  - Backscatter, glint and CBET
  - Preheat (mainly inner shell)





# Capsule ablator asymmetries arise from thickness variations and non-closure/alignment of equatorial joint

FABRICATION

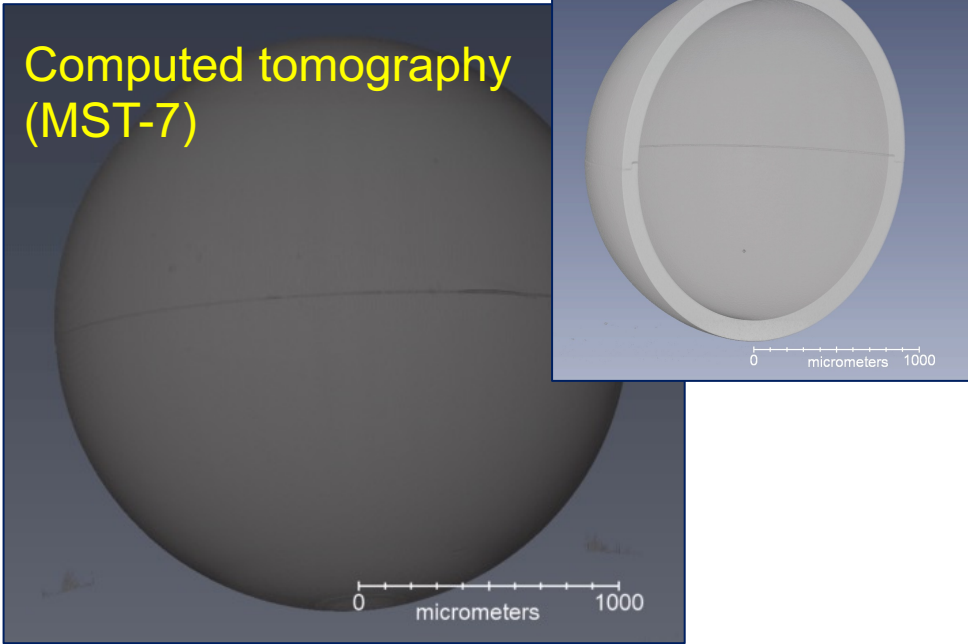


- Al hemi-shells are diamond turned to ~300 nm surface precision
- Registration of inner to outer surface can only be controlled to ~2  $\mu\text{m}$

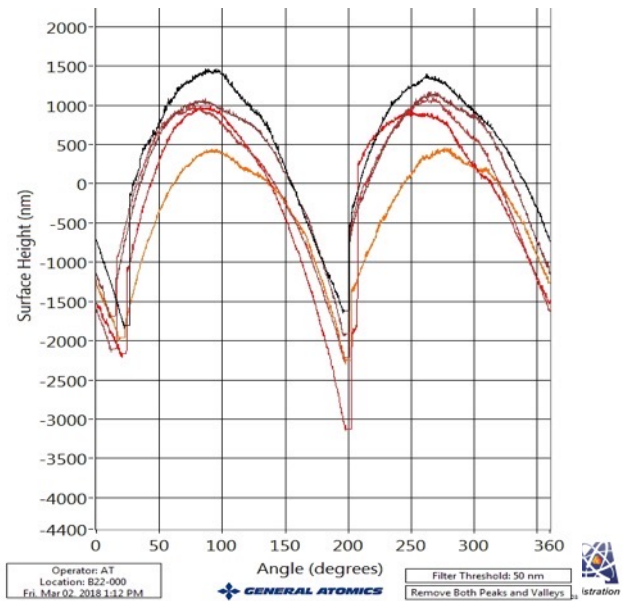
## Ablator asymmetry sources/sensitivities

- Hemi-shell outer/inner surface machining modes
- Hemi-shell surfaces non-concentricity
- Hemi-shell assembly 3D offset (tied to joint feature)

METROLOGY



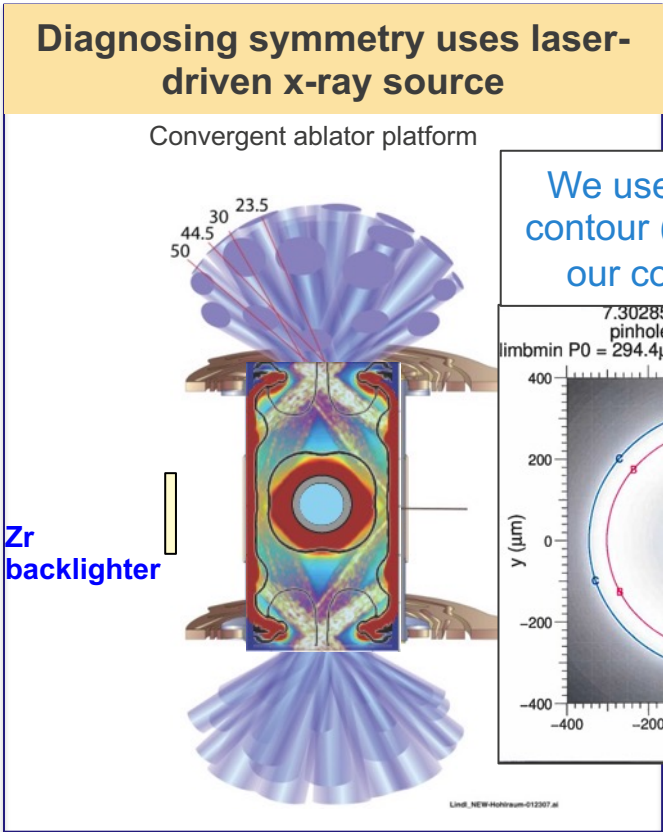
Atomic force microscopy (AFM, General Atomics) outer surface only



# We use modern physics model standards in hohlraum simulations and x-ray backlighting to assess shape

HYDRA parameter	Sensitivity studies	Postshot simulations
Au wall zones	40 A first zone	same
DCA Au opac.	yes	yes
Photon group resolution (total bins)	120	85 (180 underway)
Laser rays per cone	600	same
Laser power multiplier	0.94	0.94
Non-local e <sup>-</sup> transport	Used	Flux limited (non-local underway)
Self consistent MHD	Not used	Not used
Inline CBET	Not yet used	Not yet used
Angular zoning (degrees/zone)	1	same

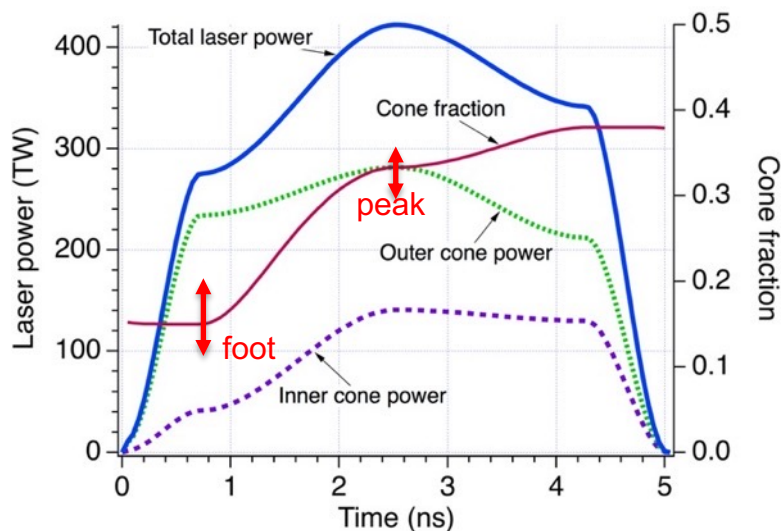
O.S. Jones et al., Phys. Plasmas 24, 056312 (2017)  
Farmer et al. Plasma Phys Control Fus. 60 (2018).



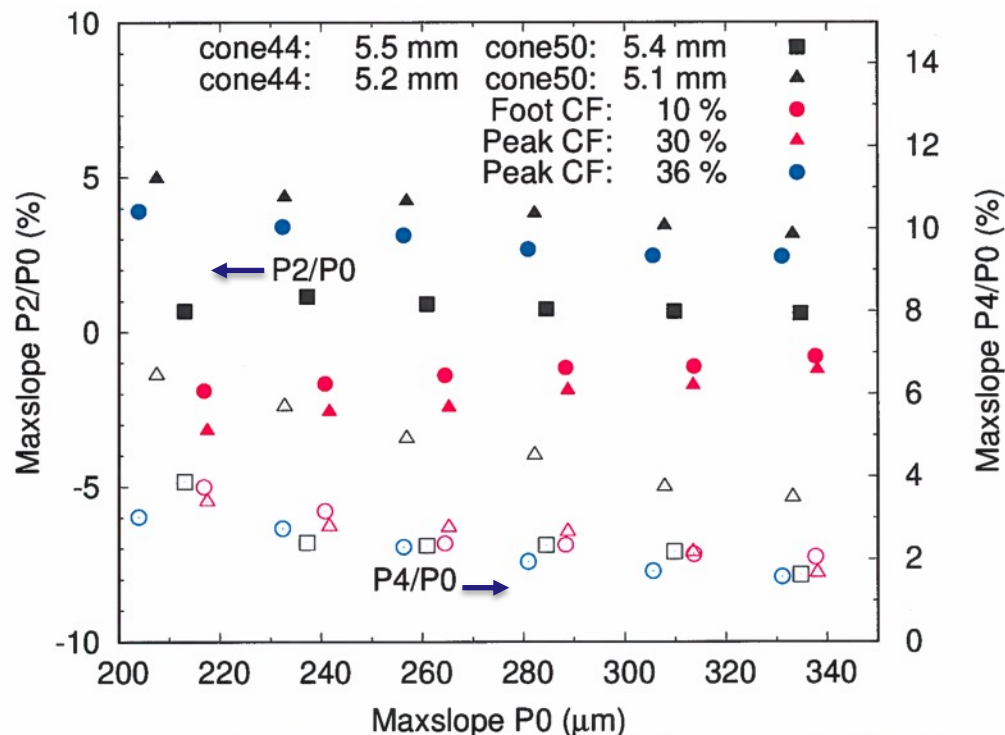
J.R. Rygg et al., Phys. Rev. Letts. 195001 (2014)

# Hohlraum symmetry is controlled by time-dependent cone fraction and beam pointing

Pulse shape (nominal) used in shape sensitivity studies

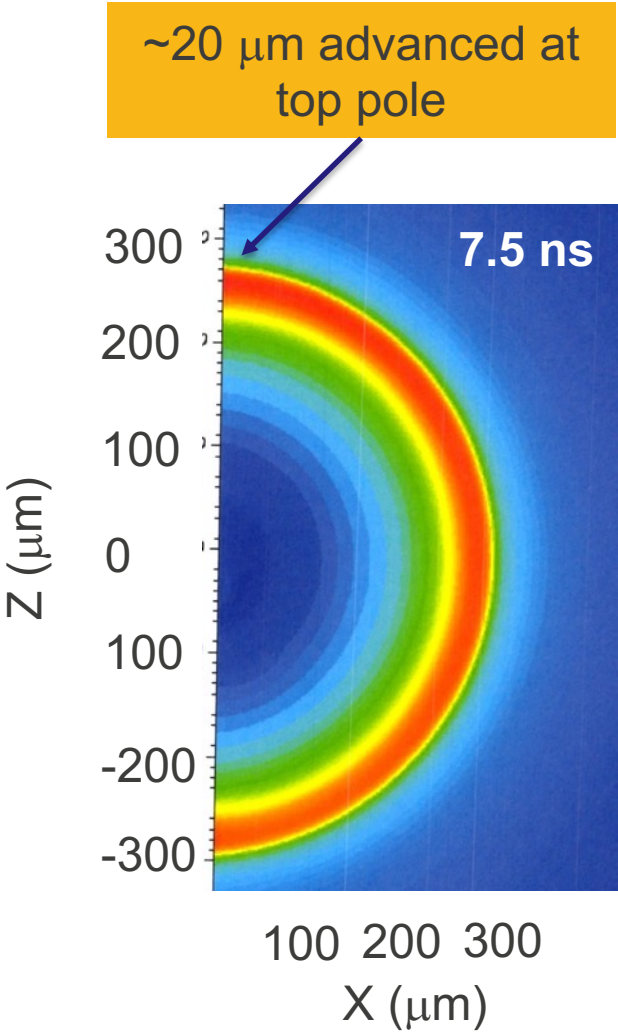
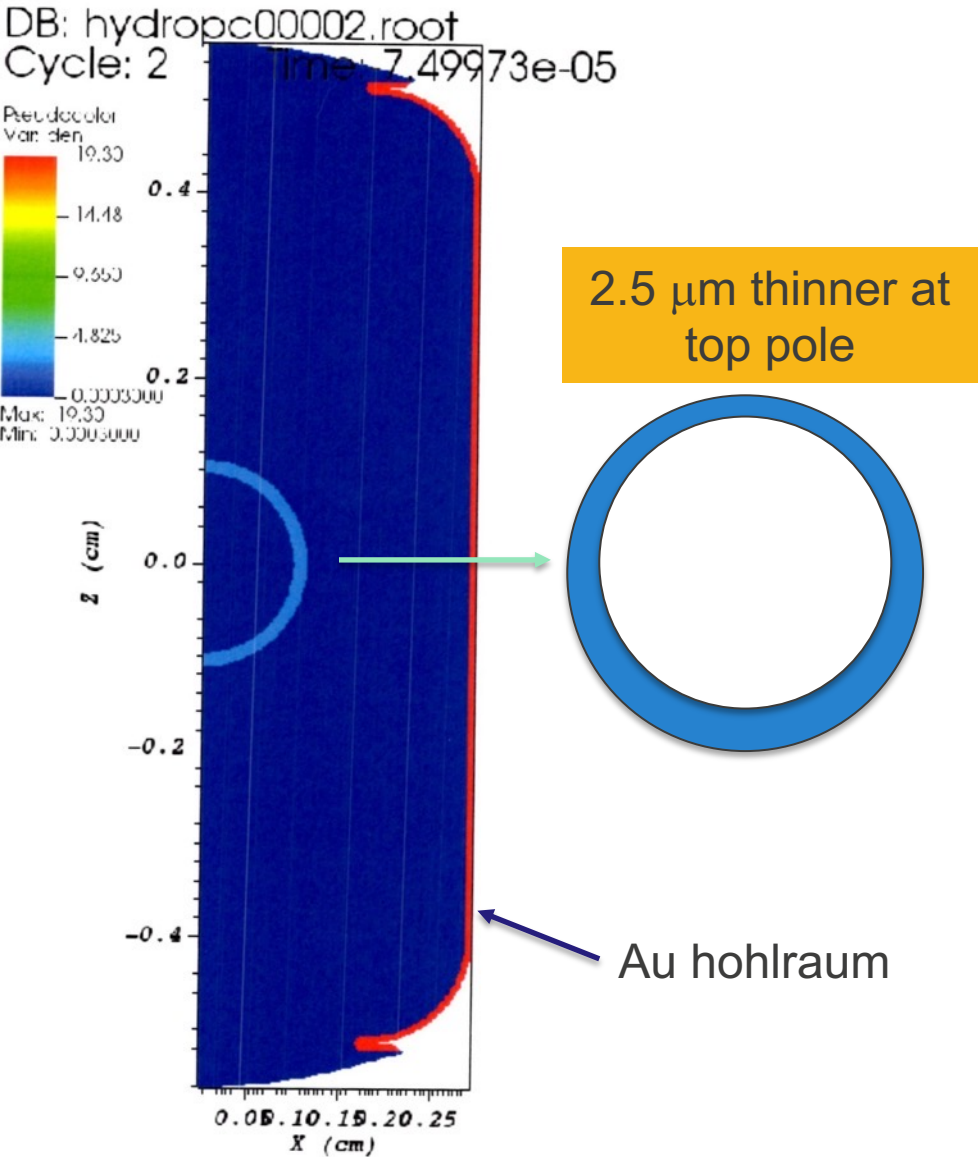


Predicted ablator P2 (closed) and P4 (open) Legendre amplitude trajectories for 145  $\mu\text{m}$  Al.  
(Black squares are nominal design)



- We predict to be near optimum 33% peak cone fraction and outer cone pointing to minimize P2, P4 in 575-scale hohlraum (case-capsule ratio = 2.6)

# Surface non-concentricity is modeled as P1 thickness variation

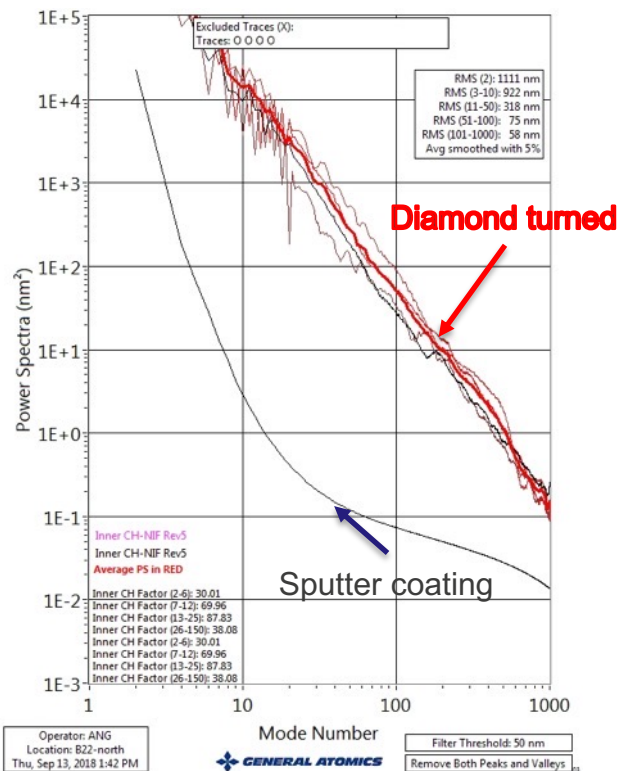


Full hohlraum radiation smoothing turned on

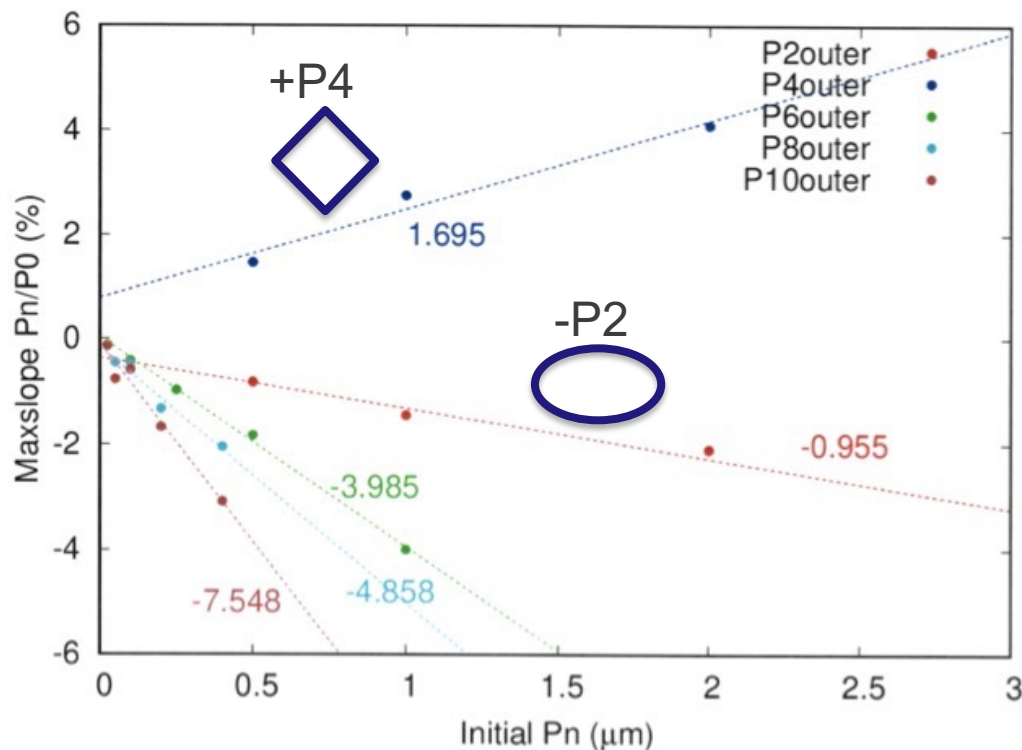


# Machined surface spectra motivates the need for outer and inner surface mode sensitivity studies

Diamond turned Al shell outer surface spectra show higher amplitudes than sputter coated shells



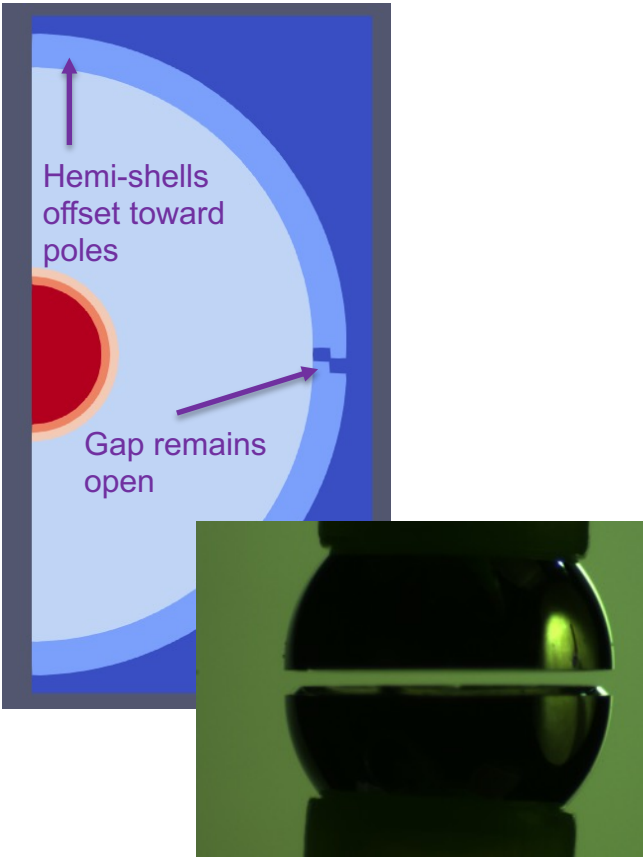
Increasing mode number leads to higher growth factors for outer surface (even) modes 2-10



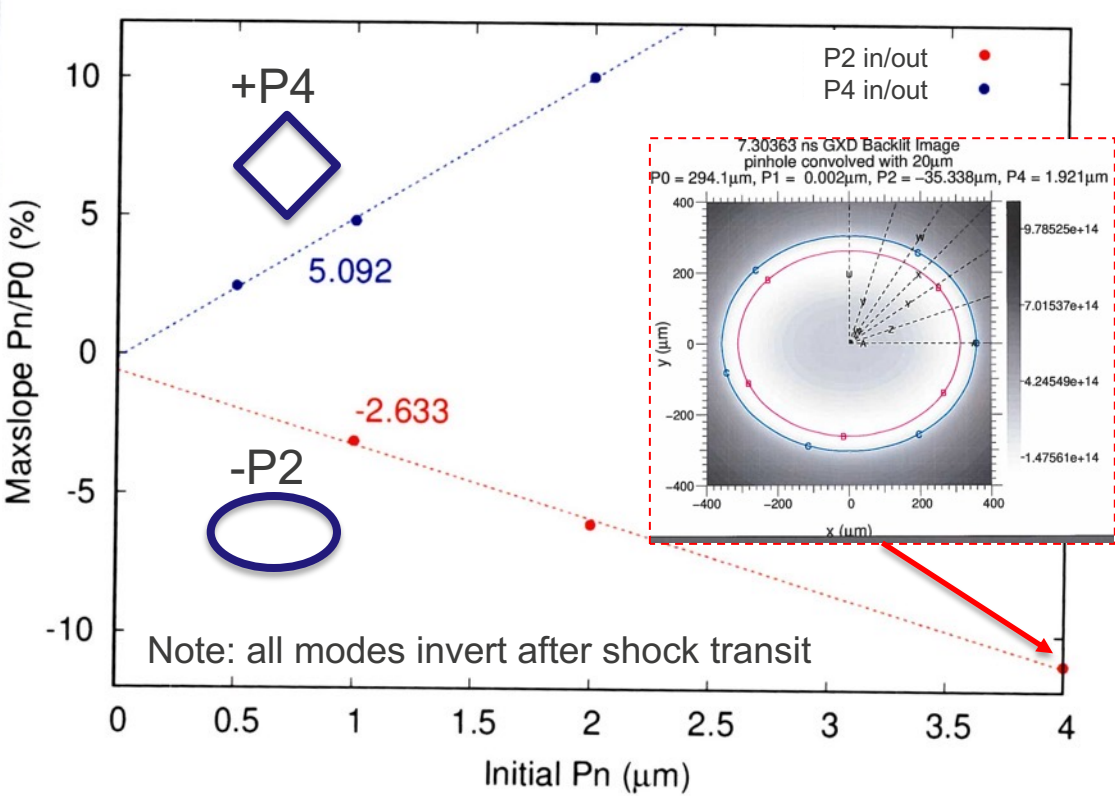
- Higher low-mode power relative to sputter coating comes from non-closure of joint gap (see next slide)
- Recent fabrication improvements have substantially reduced gap closure along with low modes (see backup slides 23 and 24)

# Non-closure of equatorial gap is a dominant source of low-modes in surface spectra

Bulk ablator shape non-uniformities may arise during assembly due to joint misfits or other assembly procedures



Predicted sensitivity to bulk ablator shape modes when same perturbation is placed on both inner and outer surface

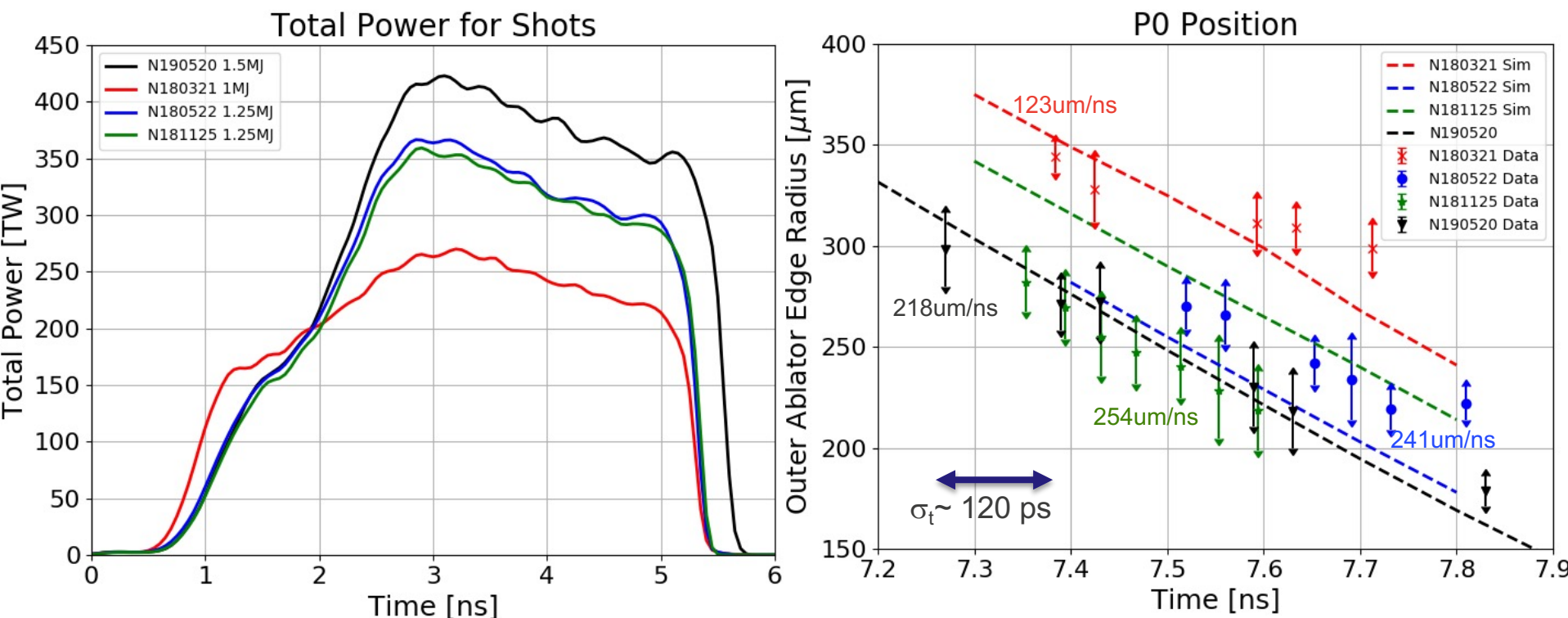


# Postshot modeling of experimental data



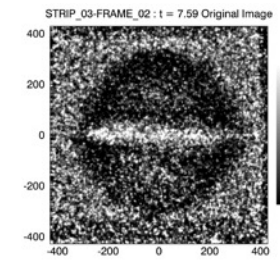
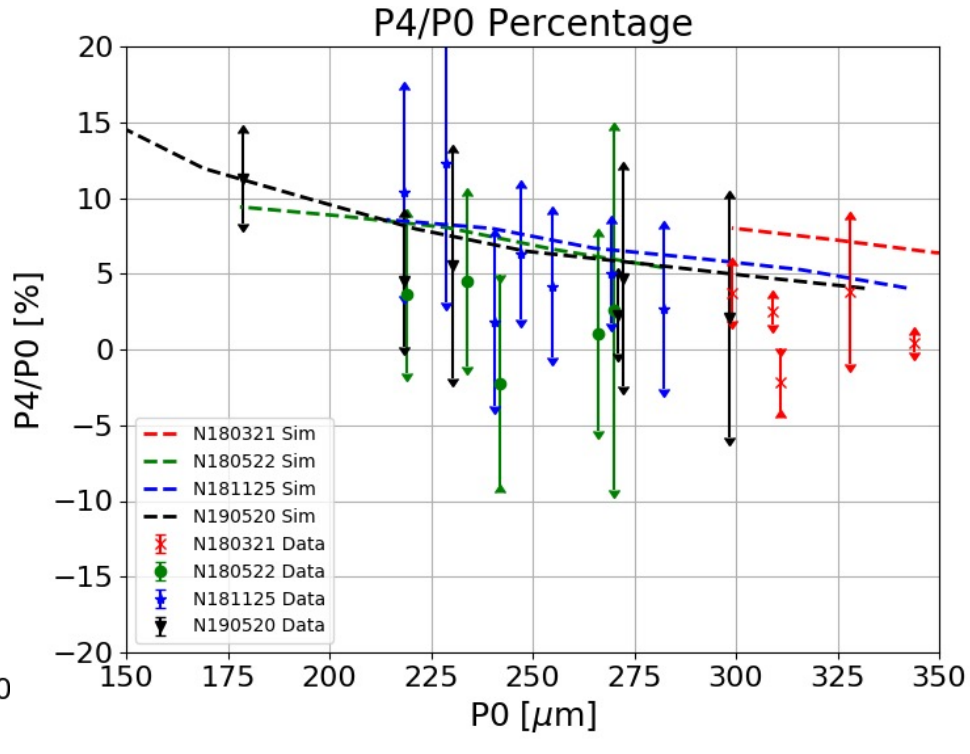
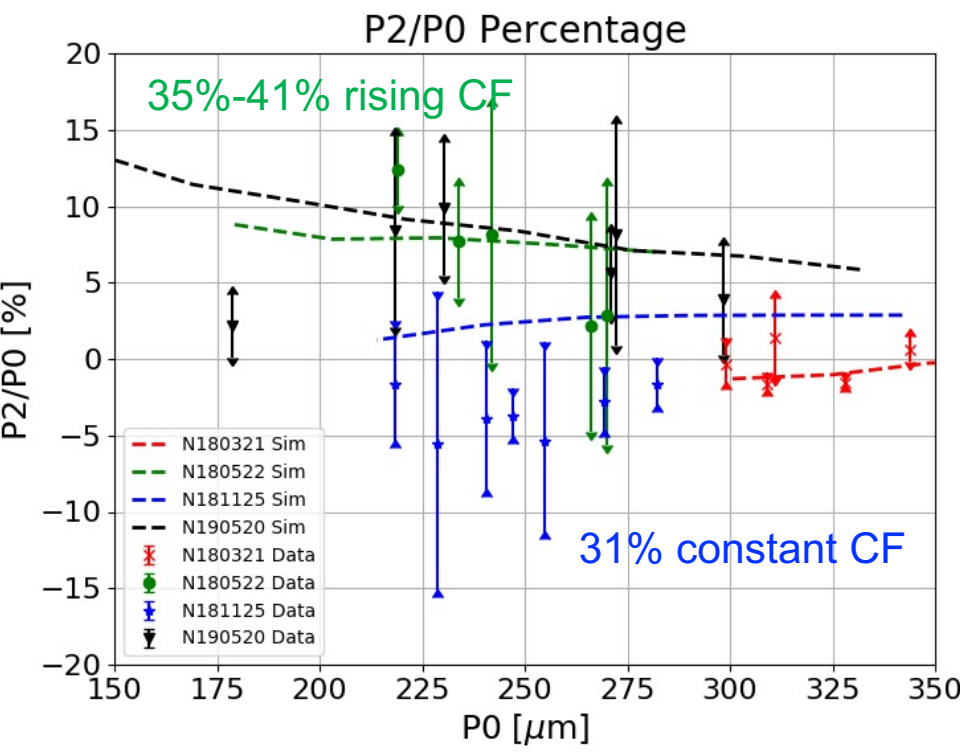
# Simulated trajectories are within 0.15 ns of measurements with discrepancies possibly due to capsule fabrication\*

\*Non-closure of joint gap

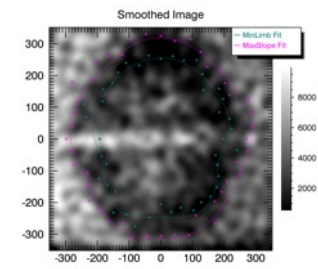


Backscatter on each shot has been <2% (see backup slides)

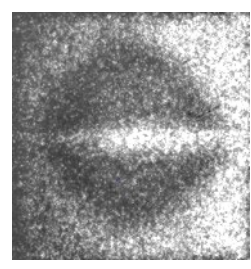
# Simulated shape is generally in line with data, and changes in cone fraction predict the direction of the P2 change



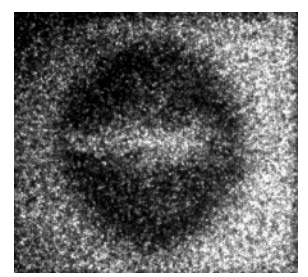
N180321



N180522



N181125



N190520

- 2DconA ablators used sub-scale thickness and had non-zero gap opening (see backup metrology slides 19-22)

# Conclusions and next steps

- **Sensitivity studies of identified asymmetry sources**
  - Inward pointing of outer cones by 300  $\mu\text{m}$  increases P4/P0 by 2%
  - 4% change in P2/P0 observed for cone fraction change between 30-36%
  - $\sim 1 \mu\text{m}$  P1 thickness variation leads to  $\sim 3\%$  P1/P0 at collision time
  - Outer and inner surface modes show increasing growth rate up to imposed P10
- **Quantification of control**
  - Measured P2 shift due to designed cone fraction change was in qualitative agreement with HYDRA postshot simulations
  - Need to confirm that lack of quantitative agreement with N181125 is due to capsule fabrication artifacts
- **Better control currently limited by ablator fabrication**
  - Equatorial joint gap closure to  $< 1$  micron recently demonstrated
- **Continue asymmetry source assessment of point design double shell performance (L2 milestone in FY22)**

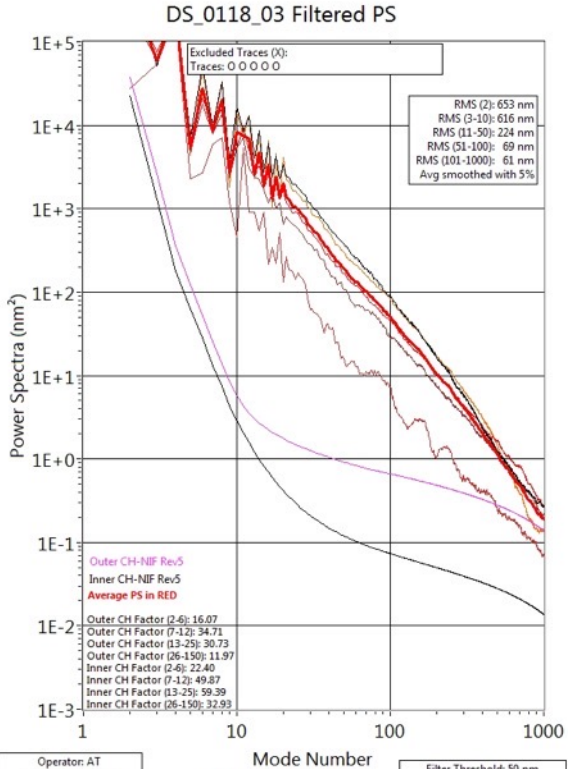
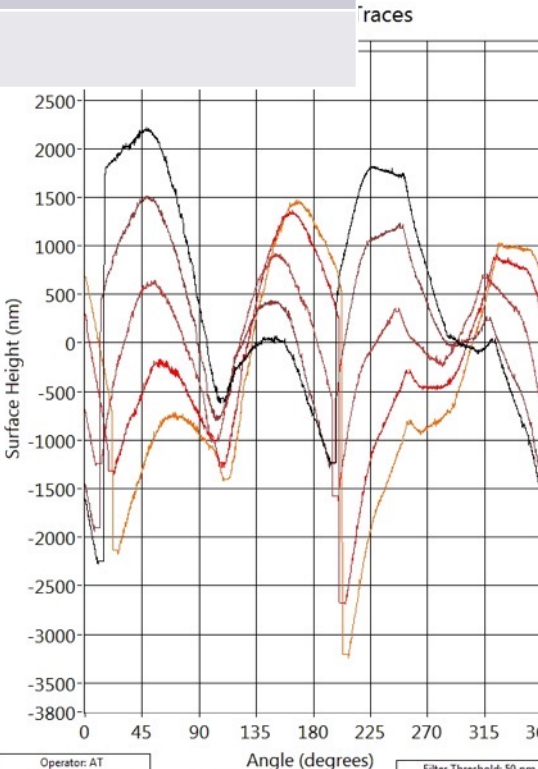
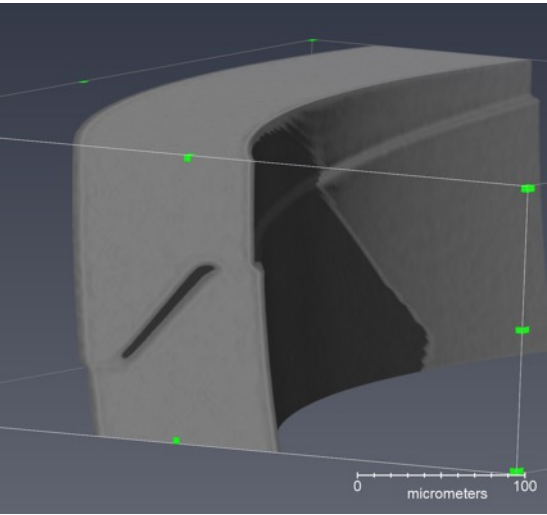
**THANK YOU!**

# Metrology for N180321-003

Dimension	measurement
Ablator thickness	106 micron
Joint gap	4-6 micron
Joint offset/step	?
Surface concentricity	TOP: ??? BOT: ???
Hohlraum length	
LEH diameter	

Compare top to bottom

Compare outer to inner



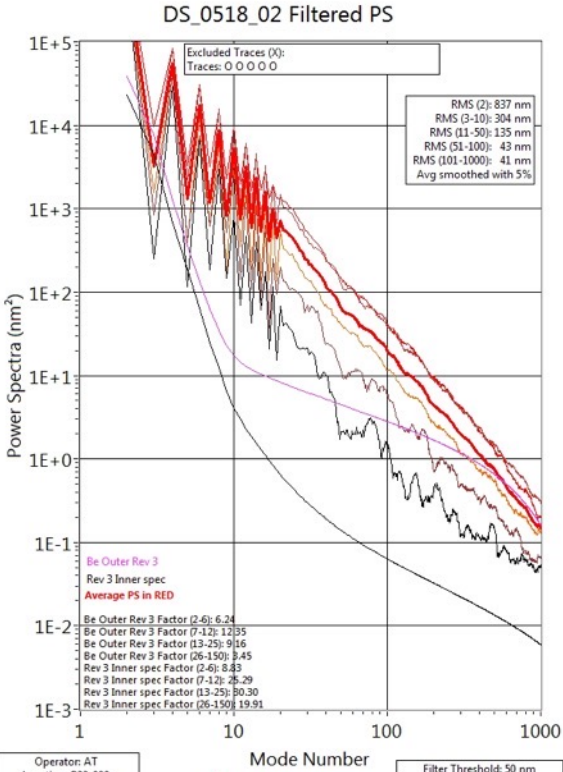
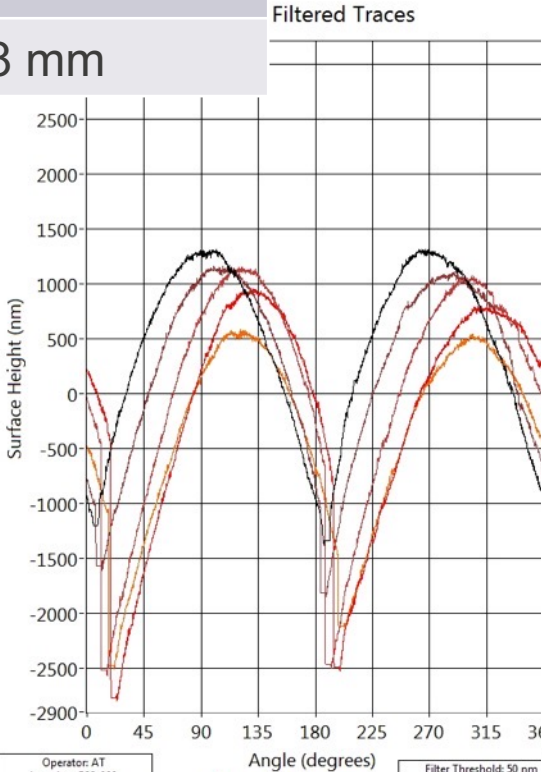
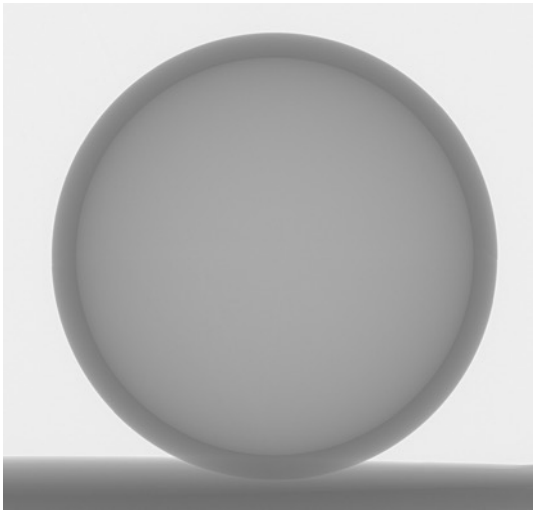


# Metrology for N180522-002

Dimension	measurement
Ablator thickness	120 micron
Joint gap	>3 um
Joint offset/step	3 um in Y
Surface concentricity	TOP: 1 um in Y BOT: 1 um in X
Hohlraum length	10.16 mm
LEH diameter	3.38 mm

Compare top to bottom x or y

Compare outer to inner



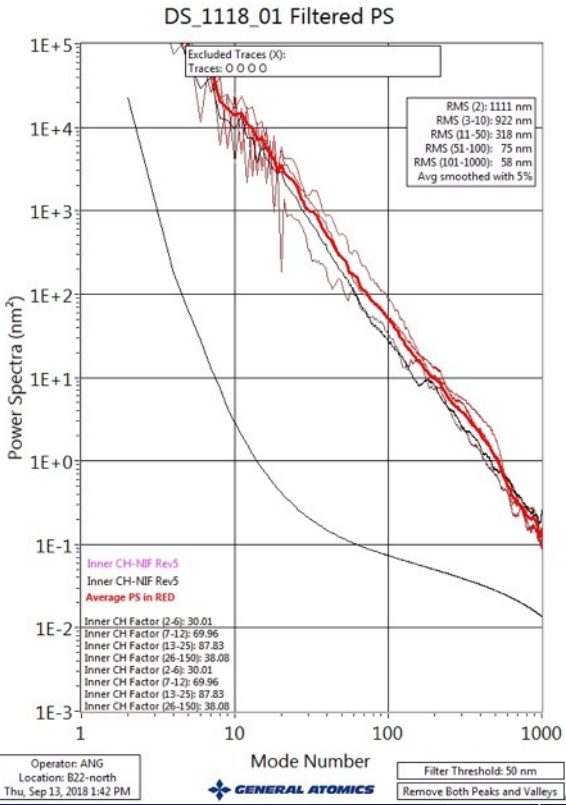
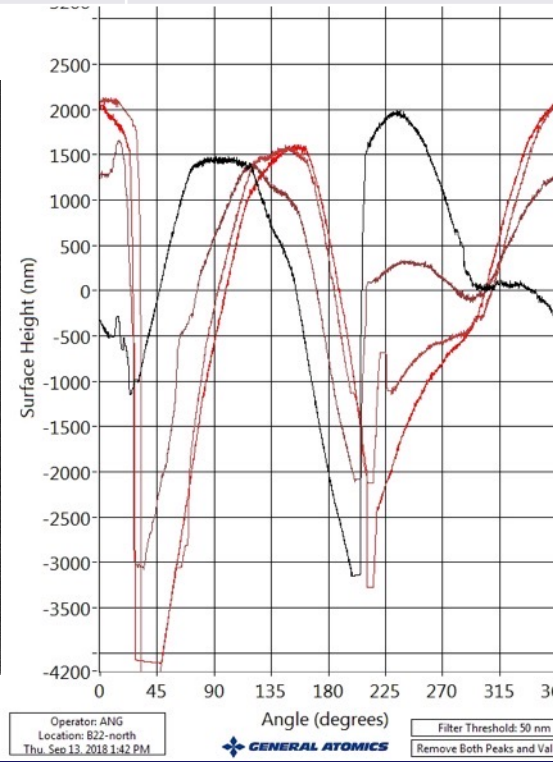
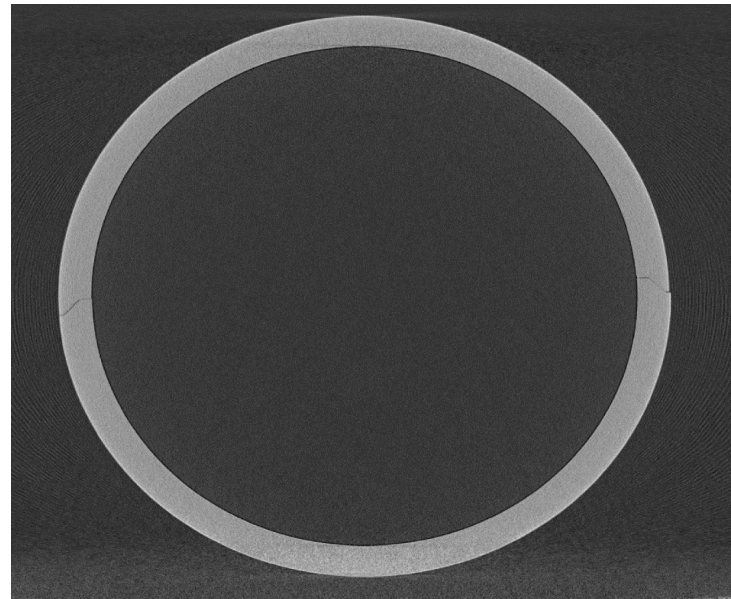
# Metrology for N181125-003

Dimension	Capsule 1	Capsule 2
Ablator thickness	120 micron	
Joint gap	5 micron	Below CT
Joint offset/step	3-6 um in X	4 micron in Y
Surface concentricity	TOP: 2 um vert BOT: 3 um horz	TOP: 0-1 um BOT: 3 um vert
Hohlraum length		
LEH diameter		

Started using Keyence IM

Compare top to bottom

Compare outer to inner



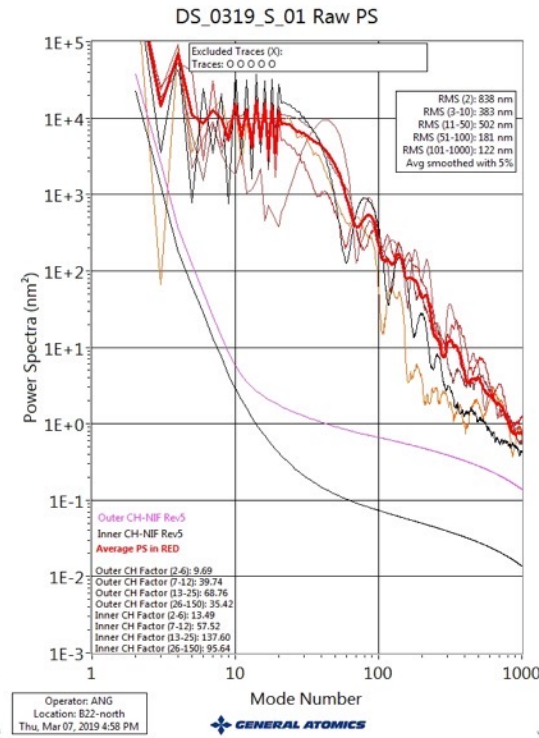
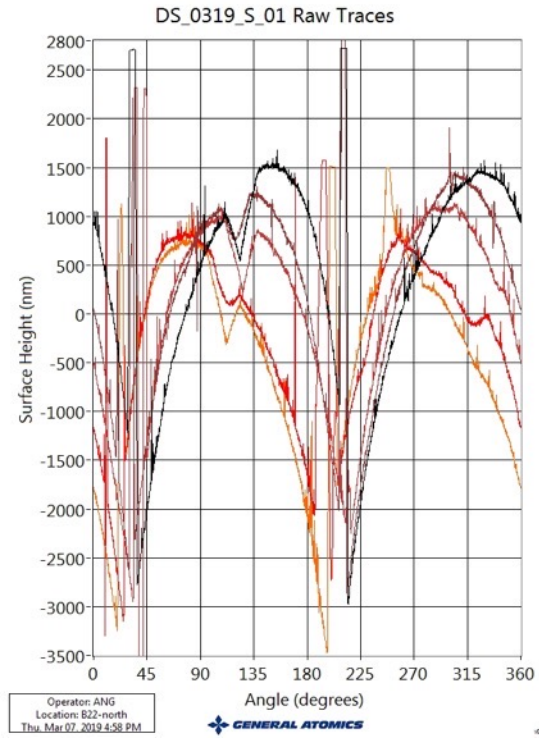
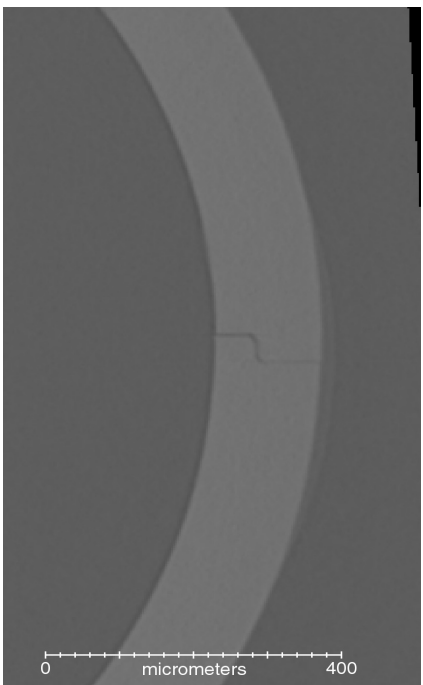


# Metrology for N190520-002

Dimension	Capsule 1
Ablator thickness	128 micron
Joint gap	7-10um
Joint offset/step	1-2 um in X
Surface concentricity	TOP: 2 um in X, Y BOT: 1 um in X
Hohlraum length	10.13 mm
LEH diameter	3.38 mm

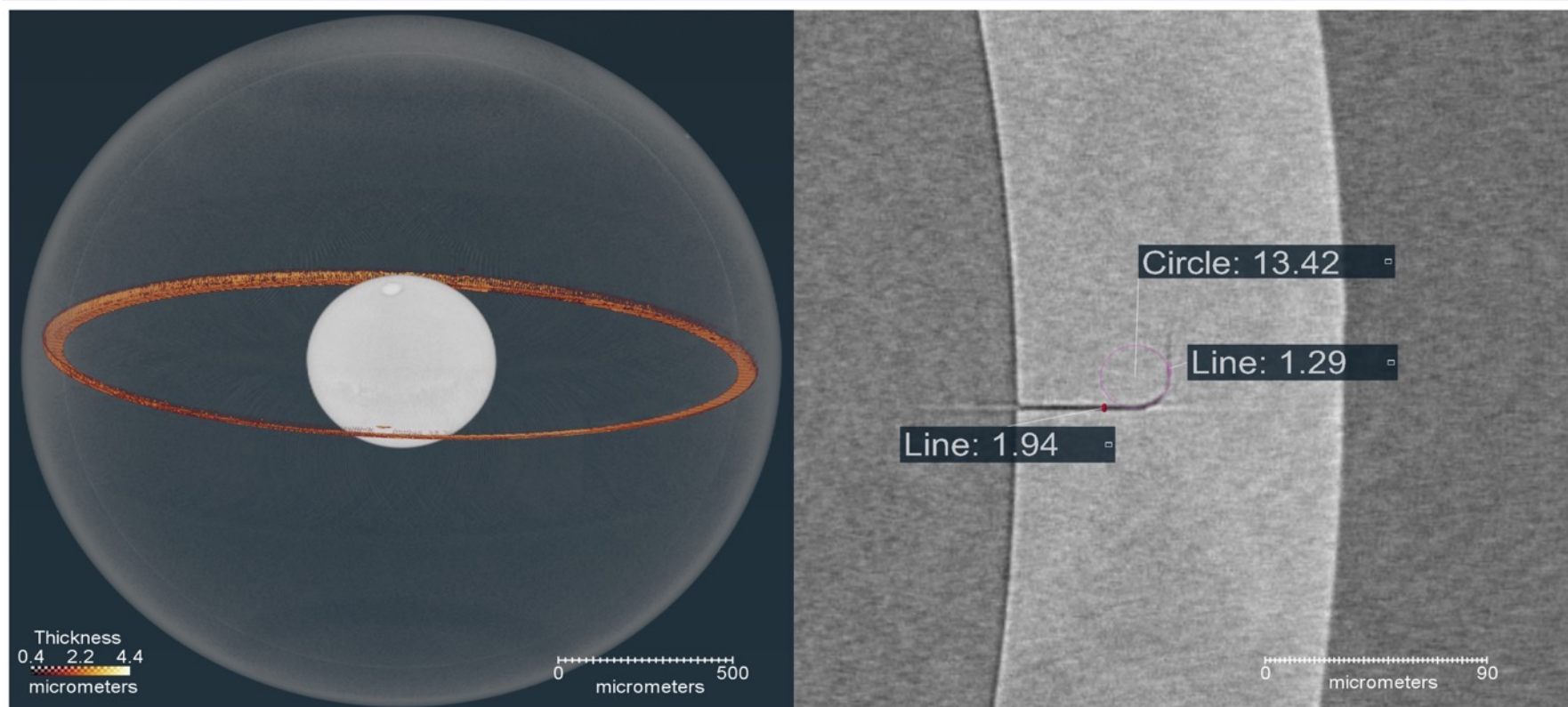
Compare top to bottom x or y

Compare outer to inner

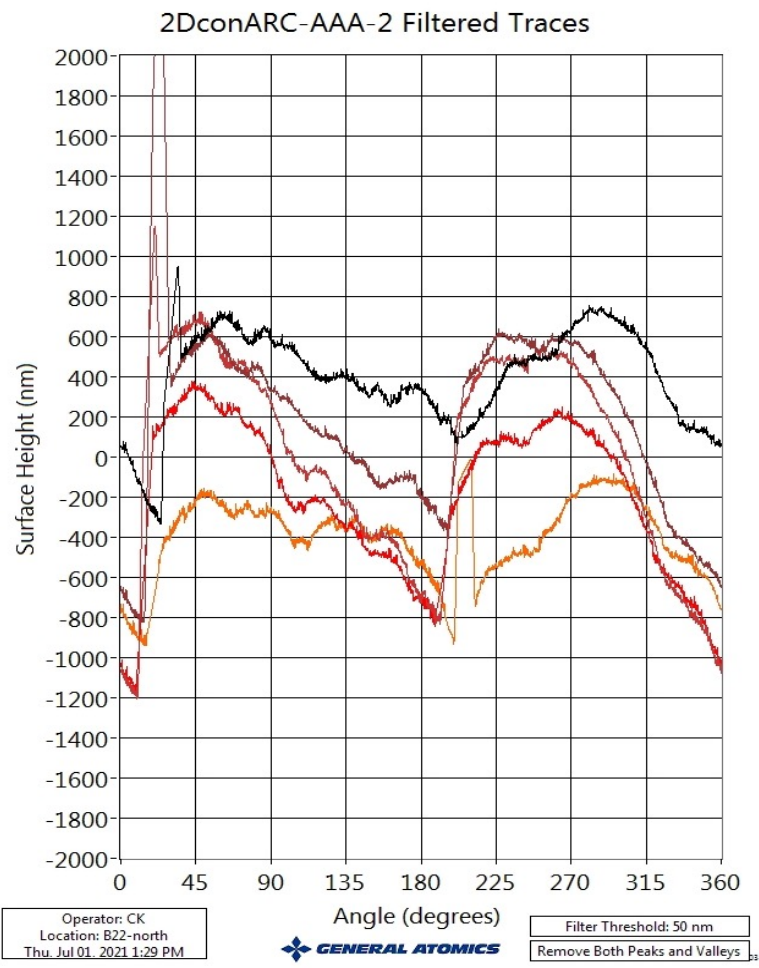
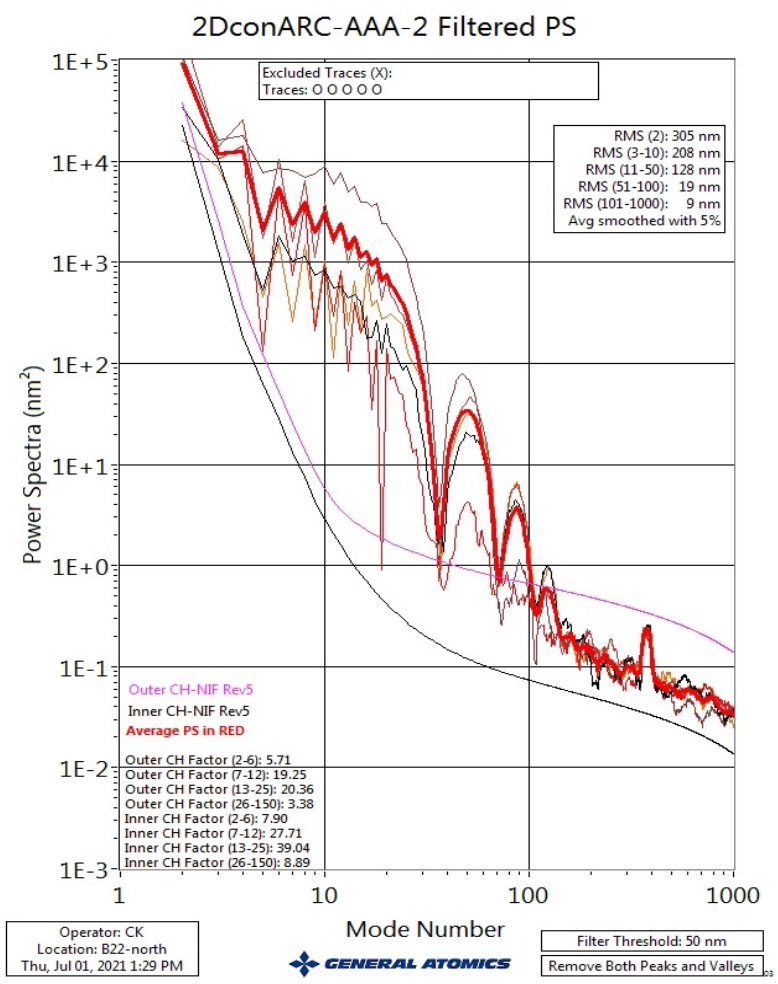


# Improved fabrication is significantly reducing joint gap closure and ablator surface modes

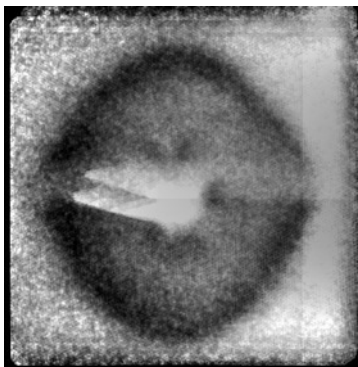
## AAA-2 Joint thickness



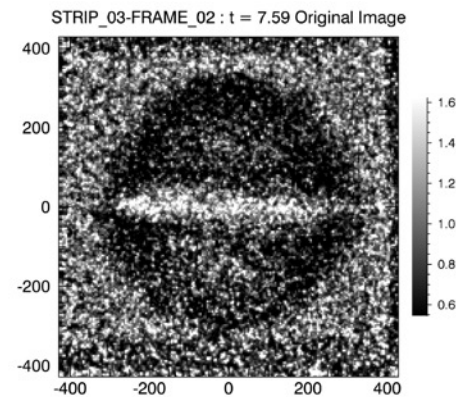
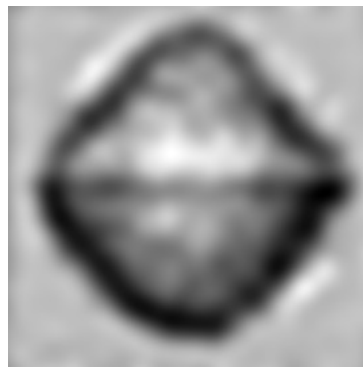
# Improved fabrication is significantly reducing joint gap closure and ablator surface modes



- Note N180321-003 was first shot moving to reduced P4 by shifting outer cone pointing, increasing hohlraum length, and reducing LEH size. Perhaps is useful to show N170322-001 image for comparison



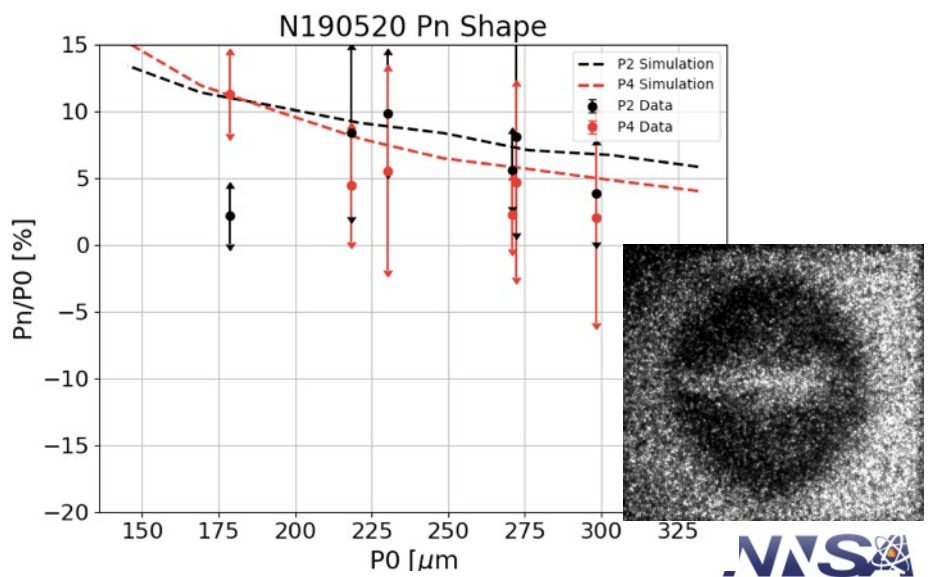
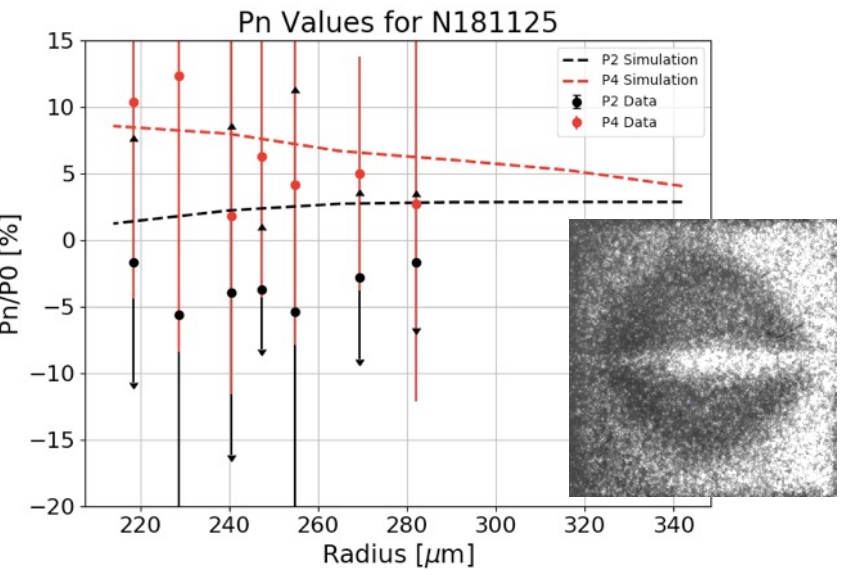
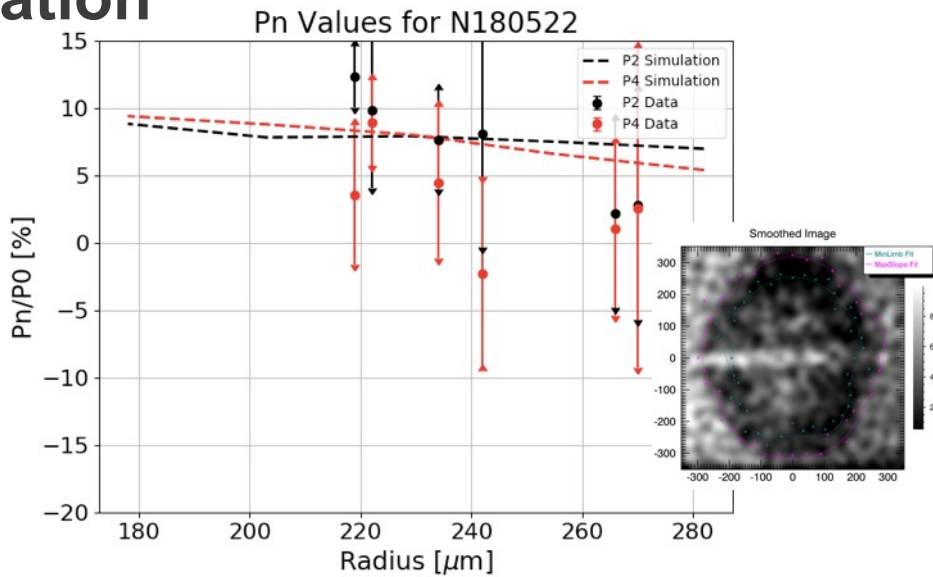
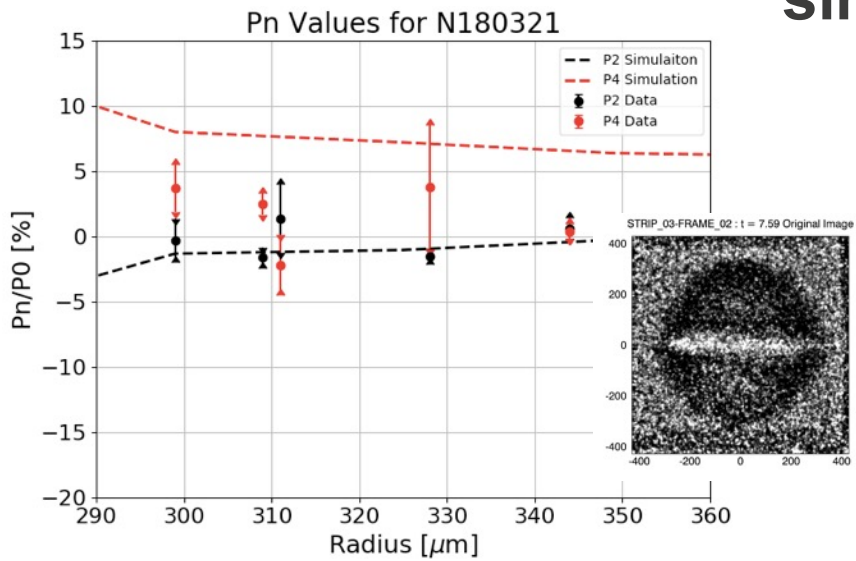
2017



2018-current



# Shape values for each experiment show that there is still progress to be made in reconciling experiment and simulation



# The root mean square deviation (RMSD) gives a quantitative measure of how much experiment and simulation differ

- The RMSD is calculated by comparing the difference between experimental and simulated data points using the formula

$$RMSD = \sqrt{\frac{\sum_{i=1}^N (x_i - \hat{x}_i)^2}{N}}$$

- $x_i$  is the experimental value,  $\hat{x}_i$  is the simulated value, and N is the number of experimental data points.
- Here predictability is defined as the RMSD being less than the average experimental error for a given measurement.

Shot	P0 RMSD [μm]	P0 Average Error [μm]	P2 RMSD [μm]	P2 Average Error [μm]	P4 RMSD [μm]	P4 Average Error [μm]
N180321	17.67	11.71	4.68	4.08	19.70	6.53
N180522	25.08	13.36	8.94	15.0	13.80	18.16
N181125	48.90	17.95	17.20	10.86	7.54	13.60
N190520	9.82	15.62	7.79	10.81	6.57	13.59

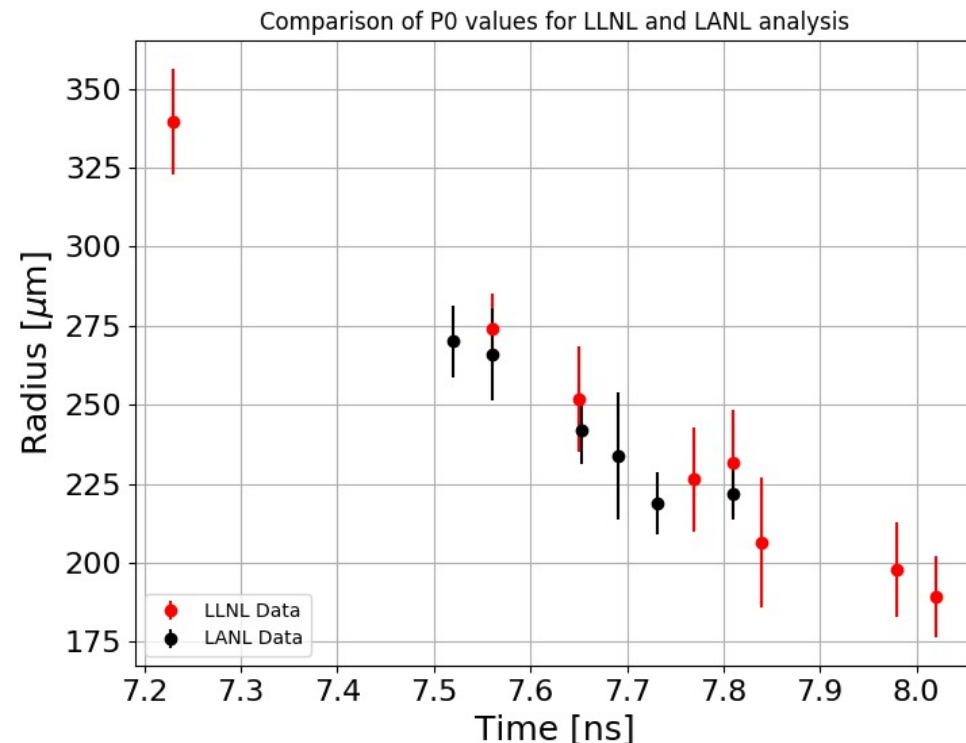
# Uncertainty estimation in shape analysis (Shahab Khan, LLNL)

- **Statistical**

- Variations of the amplitudes found from decomposition of each image within a filter

- **Systematic**

- Quadrature sum of correlation, subtraction, and smoothing errors
- Correlation: small translations of the image comparing resulting shape metrics
- Subtraction: varying size of ellipse that defines background region
- Smoothing: increase/decrease levels of smoothing; using gaussian kernels



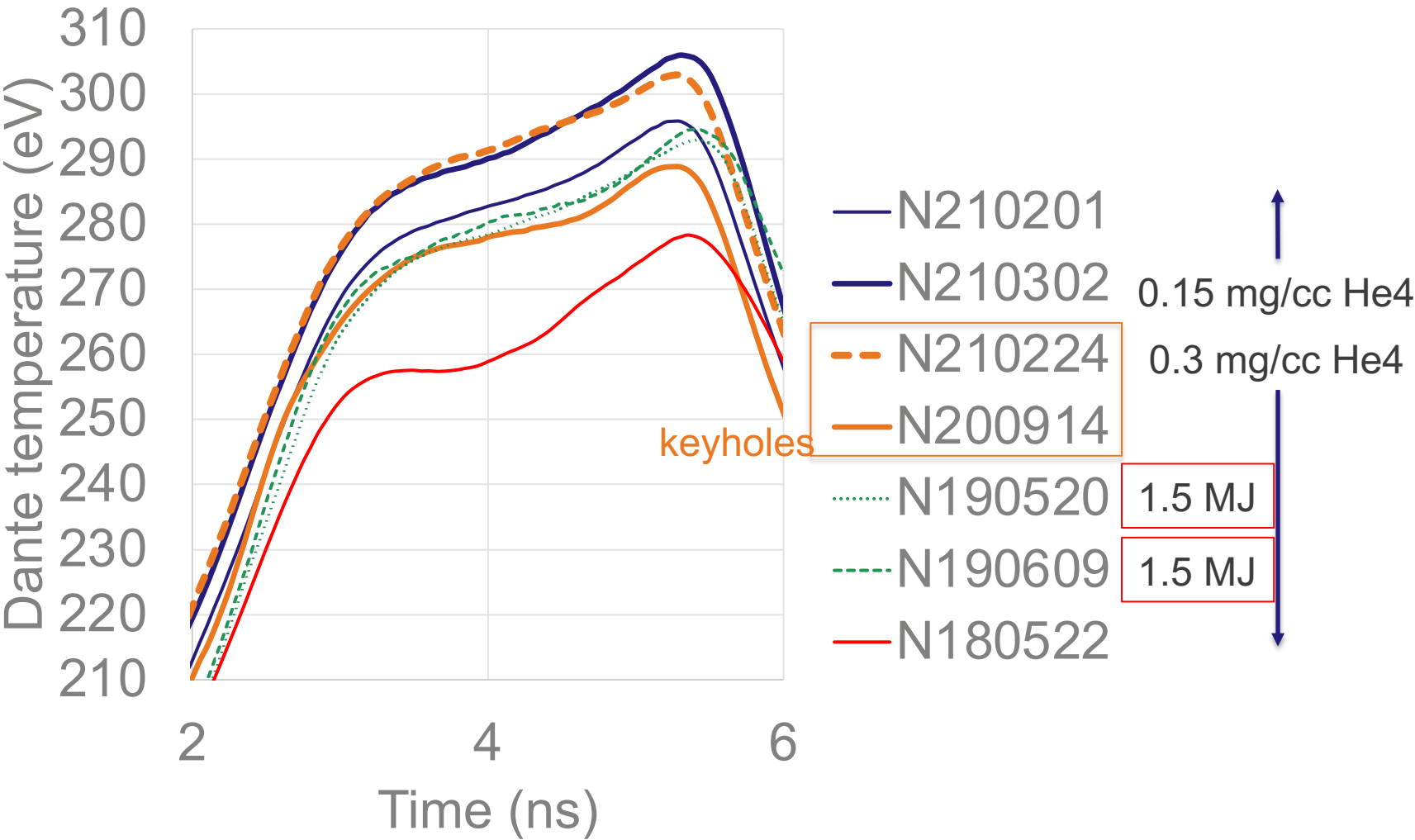


# Backscatter results

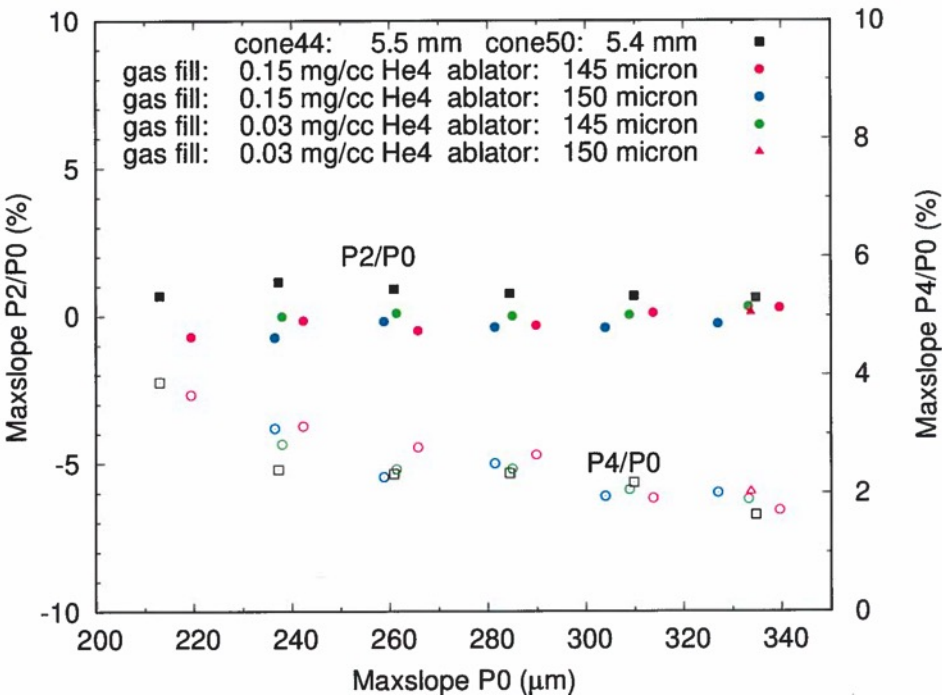
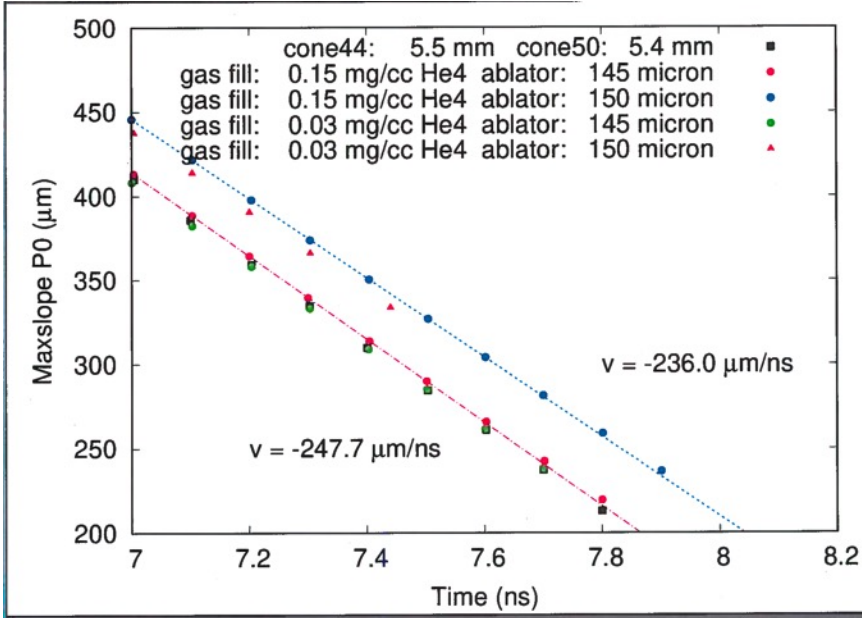
N160120-001 Be capsule			N160313-002 Be capsule			N170222-003 Al capsule			N170322-001 Al capsule		
Cone	Quad Estimate (kJ)	Cone Estimate (kJ)	Cone	Quad Estimate (kJ)	Cone Estimate (kJ)	Cone	Quad Estimate (kJ)	Cone Estimate (kJ)	Cone	Quad Estimate (kJ)	Cone Estimate (kJ)
23 deg. SRS		0.4	23 deg. SRS	0.03	0.24	23 deg. SRS	0.01	0.11	23 deg. SRS	0.02	0.12
23 deg. SBS		0	23 deg. SBS	0.54	4.29	23 deg. SBS	0.16	1.25	23 deg. SBS	0.15	1.21
30 deg. SRS		8.82E-03	30 deg. SRS	0.03	0.25	30 deg. SRS	0.03	0.27	30 deg. SRS	0.02	0.13
30 deg. SBS		0.19	30 deg. SBS	0.54	4.29	30 deg. SBS	0.16	1.25	30 deg. SBS	0.15	1.21
50 deg. SRS		0.01	50 deg. SRS	8.76E-03	0.14	50 deg. SRS	8.16E-03	0.13	50 deg. SRS	8.14E-03	0.13
50 deg. SBS		0.17	50 deg. SBS	0.06	1.02	50 deg. SBS	0.08	1.28	50 deg. SBS	0.07	1.16
44 deg. SRS		0.01	44 deg. SRS	8.76E-03	0.14	44 deg. SRS	8.16E-03	0.13	44 deg. SRS	8.14E-03	0.13
44 deg. SBS		0.17	44 deg. SBS	0.01	0.22	44 deg. SBS	0.02	0.28	44 deg. SBS	0.02	0.26
Total Backscatter (kJ)		0.97	Total Backscatter (kJ)		10.6	Total Backscatter (kJ)		4.69	Total Backscatter (kJ)		4.34
Laser Energy (kJ)		1021.86	Laser Energy (kJ)		994.43	Laser Energy (kJ)		1015.83	Laser Energy (kJ)		1010.27
Coupling		99.9	Coupling		98.93	Coupling		99.54	Coupling		99.57
N171016-001 Al capsule			N180321-003 Al capsule			N180731-002 Al capsule			N180918-001 Al capsule		
Cone	Quad Estimate (kJ)	Cone Estimate (kJ)	Cone	Quad Estimate (kJ)	Cone Estimate (kJ)	Cone	Quad Estimate (kJ)	Cone Estimate (kJ)	Cone	Quad Estimate (kJ)	Cone Estimate (kJ)
23 deg. SRS	0.03	0.25	23 deg. SRS	0.04	0.31	23 deg. SRS	0.04	0.28	23 deg. SRS	0.03	0.24
23 deg. SBS	0.07	0.53	23 deg. SBS	5.74E-03	0.05	23 deg. SBS	8.61E-03	0.07	23 deg. SBS	0.03	0.26
30 deg. SRS	0.04	0.31	30 deg. SRS	0.05	0.41	30 deg. SRS	0.03	0.27	30 deg. SRS	0.04	0.3
30 deg. SBS	0.07	0.53	30 deg. SBS	0.07	0.53	30 deg. SBS	0.07	0.56	30 deg. SBS	0.06	0.49
50 deg. SRS	8.87E-03	0.14	50 deg. SRS	7.74E-03	0.12	50 deg. SRS	8.60E-03	0.14	50 deg. SRS	8.21E-03	0.13
50 deg. SBS	0.98	15.62	50 deg. SBS	0.81	12.9	50 deg. SBS	0.84	13.38	50 deg. SBS	1.02	16.33
44 deg. SRS	8.87E-03	0.14	44 deg. SRS	7.74E-03	0.12	44 deg. SRS	8.60E-03	0.14	44 deg. SRS	8.21E-03	0.13
44 deg. SBS	0.21	3.44	44 deg. SBS	0.18	2.84	44 deg. SBS	0.18	2.94	44 deg. SBS	0.22	3.59
Total Backscatter (kJ)		20.97	Total Backscatter (kJ)		17.29	Total Backscatter (kJ)		17.78	Total Backscatter (kJ)		21.49
Laser Energy (kJ)		1029.78	Laser Energy (kJ)		1027.08	Laser Energy (kJ)		1045.58	Laser Energy (kJ)		1025.05
Coupling		97.96	Coupling		98.32	Coupling		98.3	Coupling		97.9

N180522 had 99%  
N190609 had 99%  
N181125 had 98%

# Better drive performance at 0.15 mg/cc fill or systematic change to Dante since FY19?

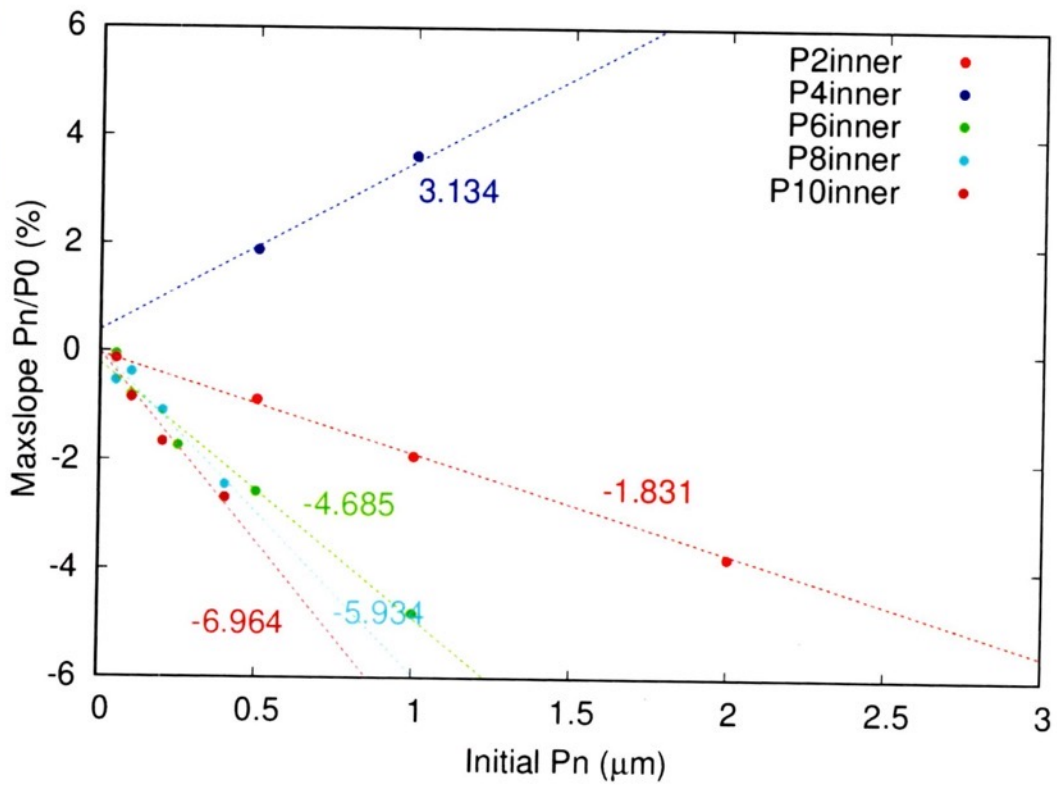
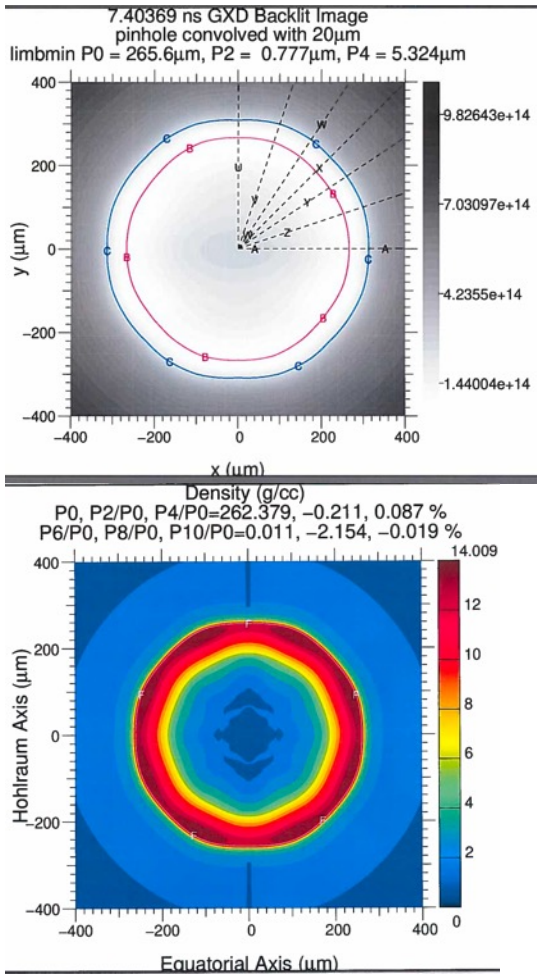


# Sensitivity to hohlraum gas fill



# HYDRA inner surface ablator mode results

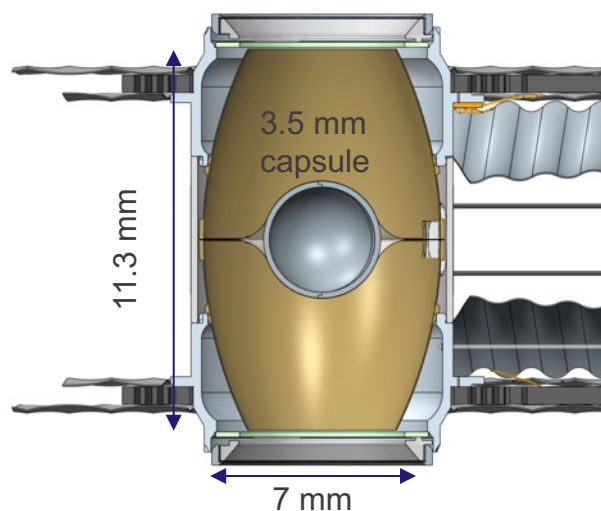
P8 mode



Inner surface modes grow moderately faster than outer surface modes

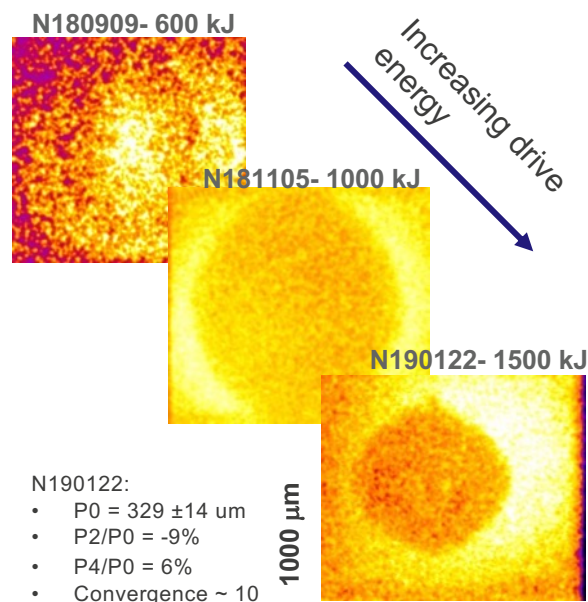
# LLNL is exploring larger scale hohlraum platforms to significantly enhance energy coupling

Advanced hohlraums are expected to couple 3-4x more energy to capsule



RI: Y. Ping, V. Smalyuk (LLNL)  
Designer: P. Amendt (LLNL)

## In-flight radiography of large outer shell

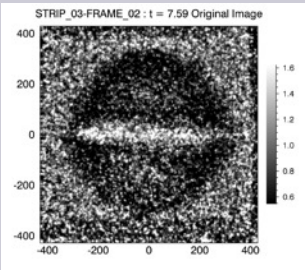
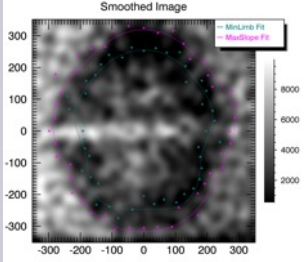
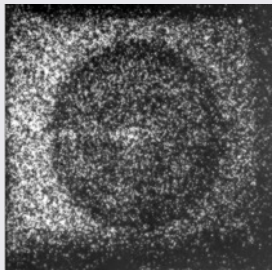
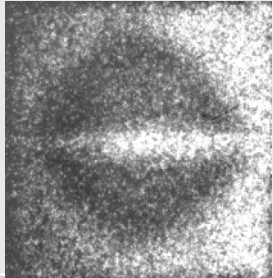
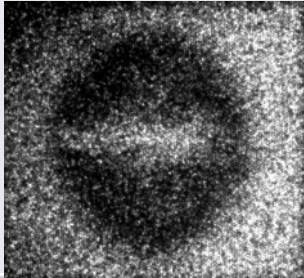
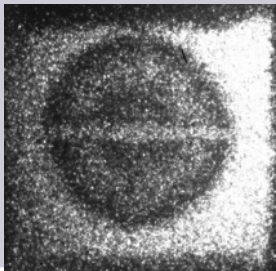
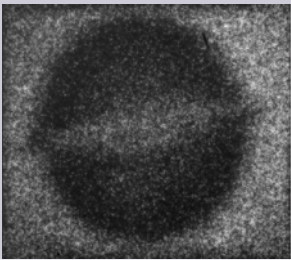


- N190122:
- $P_0 = 329 \pm 14 \text{ } \mu\text{m}$
  - $P_2/P_0 = -9\%$
  - $P_4/P_0 = 6\%$
  - Convergence  $\sim 10$

\*Y. Ping et al., Nature Physics (2018)

# Radiography data summary

Can we analyze modes 1,2,3,4,5,6?

1 MJ	1.25 MJ	1.5 MJ
<div>N180321-003</div> <div></div>	<div>N180522-002</div> <div></div>	
<div>N180731-002</div> <div>Glass inner</div> <div></div>	<div>N181125-003</div> <div></div>	<div>N190520-002</div> <div></div>
<div>N180918-001</div> <div>Glass inner</div> <div></div>	<div>N180430-001</div> <div></div>	







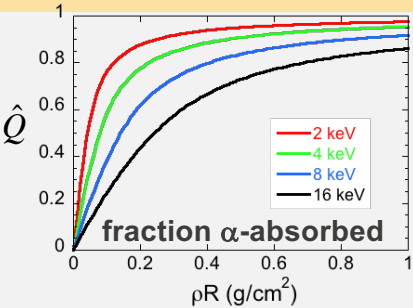
# High-Z shells offer new opportunities to assess power balance in a confined, burning plasma

\*Montgomery, Daughton et al., Phys. Plasmas 25, 092706 (2018)

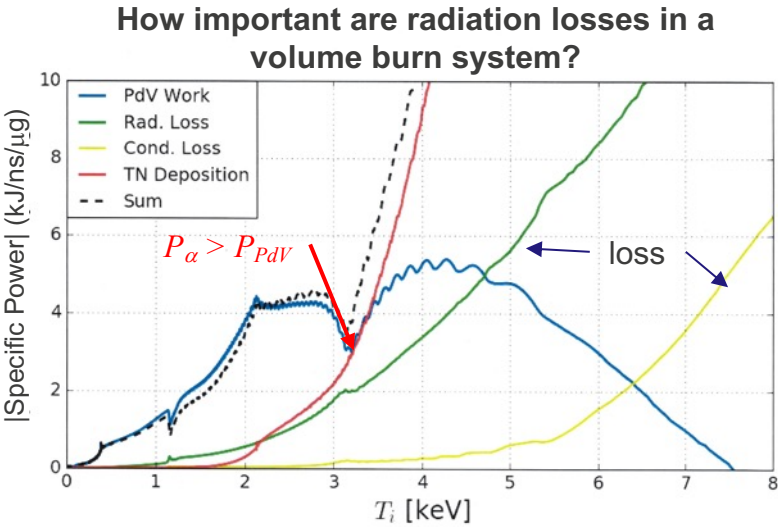
## Fusion heating rate must exceed expansion losses

$$T_{keV} > \frac{4}{\left(\rho R_* f_{tamp} \hat{Q}\right)^{0.4}}$$

- Ensures burn begins before peak compression
- ‘Robust’ to implosion asymmetries and pusher/fuel mix
- Does not include radiation losses...



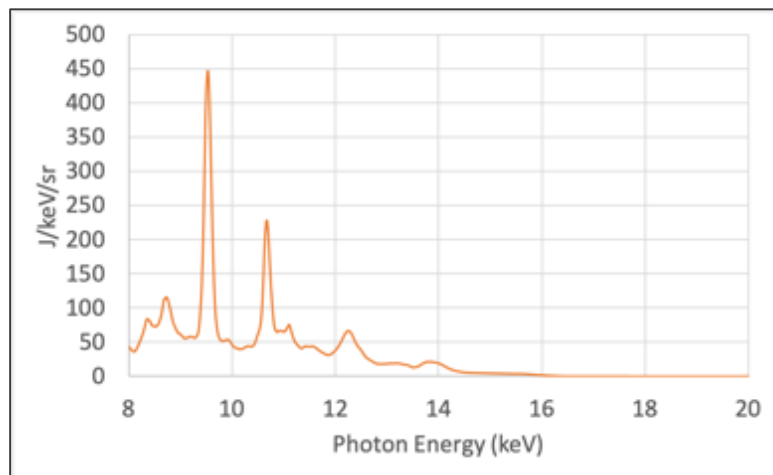
$\rho R$ (g/cm <sup>2</sup> )	T (keV)
0.25	> 4.6
0.35	> 3.9
0.60	> 3.1



Mass-averaged fuel temperature

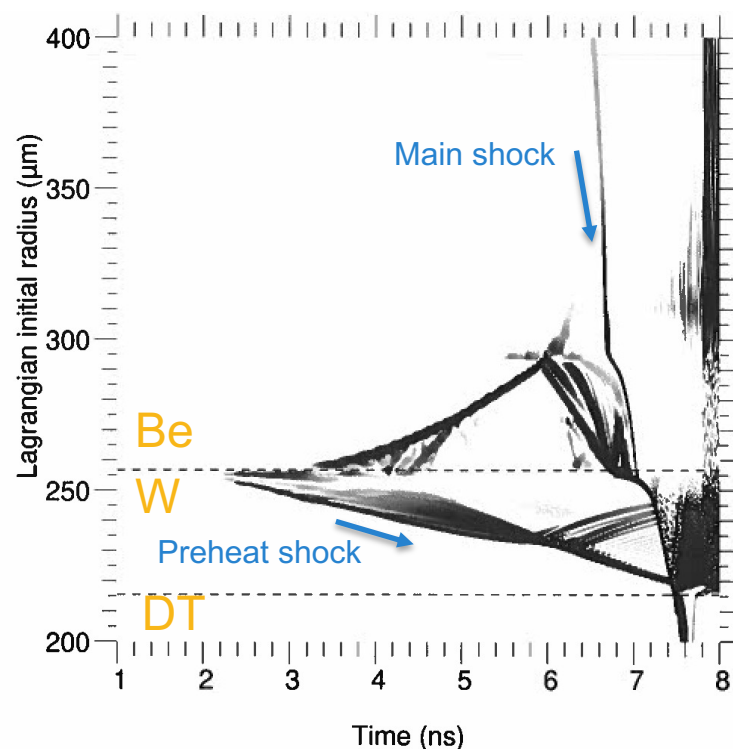
# FY20/21 keyhole experiments used to constrain shock and preheat as independent sources of asymmetry for high-Z inner shell

Au L-shell spectrum measured through LEH on keyhole shot N200914-001



NXS analysis, C. Krauland (GA)

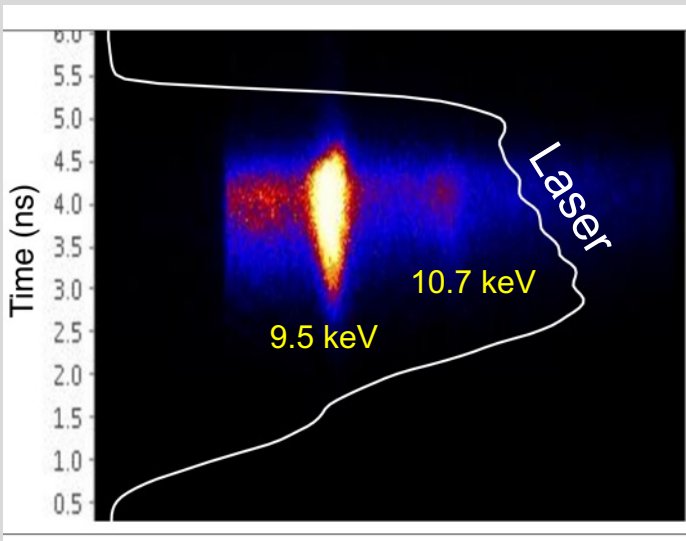
HYDRA shock trajectories in double shell point design



- Preheat (Au L-shell) and main shock set inner shell adiabat
- Accurate Au L-shell modeling requires non-local thermal conduction and nLTE DCA opacities

# February 2021 keyhole made first measurement of preheat asymmetry in a double shell

Au L-shell emission (polar NXS, Disc)  
found to turn on with high power



Raw line VISAR data showing W inner  
surface motion. **Used 20 micron W and  
20 micron Be shell**

